

A new large-bodied thalattosuchian crocodyliform from the Lower Jurassic (Toarcian) of Hungary, with further evidence of the mosaic acquisition of marine adaptations in Metriorhynchoidea (#23877)

1

First submission

Editor guidance

Please submit by **8 Mar 2018** for the benefit of the authors (and your \$200 publishing discount).



Structure and Criteria

Please read the 'Structure and Criteria' page for general guidance.



Custom checks

Make sure you include the custom checks shown below, in your review.



Raw data check

Review the raw data. Download from the [materials page](#).



Image check

Check that figures and images have not been inappropriately manipulated.

Privacy reminder: If uploading an annotated PDF, remove identifiable information to remain anonymous.

Files

Download and review all files from the [materials page](#).

12 Figure file(s)

1 Table file(s)

6 Raw data file(s)



Custom checks

New species checks



Have you checked our [new species policies](#)?



Do you agree that it is a new species?



Is it correctly described e.g. meets ICZN standard?



Structure your review

The review form is divided into 5 sections.

Please consider these when composing your review:

1. BASIC REPORTING

2. EXPERIMENTAL DESIGN

3. VALIDITY OF THE FINDINGS

4. General comments

5. Confidential notes to the editor

 You can also annotate this PDF and upload it as part of your review

When ready [submit online](#).

Editorial Criteria

Use these criteria points to structure your review. The full detailed editorial criteria is on your [guidance page](#).

BASIC REPORTING

-  Clear, unambiguous, professional English language used throughout.
-  Intro & background to show context. Literature well referenced & relevant.
-  Structure conforms to [PeerJ standards](#), discipline norm, or improved for clarity.
-  Figures are relevant, high quality, well labelled & described.
-  Raw data supplied (see [PeerJ policy](#)).

EXPERIMENTAL DESIGN

-  Original primary research within [Scope of the journal](#).
-  Research question well defined, relevant & meaningful. It is stated how the research fills an identified knowledge gap.
-  Rigorous investigation performed to a high technical & ethical standard.
-  Methods described with sufficient detail & information to replicate.

VALIDITY OF THE FINDINGS

-  Impact and novelty not assessed. Negative/inconclusive results accepted. *Meaningful* replication encouraged where rationale & benefit to literature is clearly stated.
-  Data is robust, statistically sound, & controlled.
-  Conclusions are well stated, linked to original research question & limited to supporting results.
-  Speculation is welcome, but should be identified as such.

Standout reviewing tips

3



The best reviewers use these techniques

Tip

Support criticisms with evidence from the text or from other sources

Example

Smith et al (J of Methodology, 2005, V3, pp 123) have shown that the analysis you use in Lines 241-250 is not the most appropriate for this situation. Please explain why you used this method.

Give specific suggestions on how to improve the manuscript

Your introduction needs more detail. I suggest that you improve the description at lines 57- 86 to provide more justification for your study (specifically, you should expand upon the knowledge gap being filled).

Comment on language and grammar issues

The English language should be improved to ensure that an international audience can clearly understand your text. Some examples where the language could be improved include lines 23, 77, 121, 128 – the current phrasing makes comprehension difficult.

Organize by importance of the issues, and number your points

1. Your most important issue
2. The next most important item
3. ...
4. The least important points

Please provide constructive criticism, and avoid personal opinions

I thank you for providing the raw data, however your supplemental files need more descriptive metadata identifiers to be useful to future readers. Although your results are compelling, the data analysis should be improved in the following ways: AA, BB, CC

Comment on strengths (as well as weaknesses) of the manuscript

I commend the authors for their extensive data set, compiled over many years of detailed fieldwork. In addition, the manuscript is clearly written in professional, unambiguous language. If there is a weakness, it is in the statistical analysis (as I have noted above) which should be improved upon before Acceptance.

A new large-bodied thalattosuchian crocodyliform from the Lower Jurassic (Toarcian) of Hungary, with further evidence of the mosaic acquisition of marine adaptations in Metriorhynchoidea

Attila Ősi ^{Corresp., 1, 2}, Mark T Young ³, András Galász ¹, Márton Rabi ^{4, 5}

¹ Department of Paleontology, Eötvös University, Budapest, Hungary

² Department of Paleontology and Geology, Hungarian Natural History Museum, Budapest, Hungary

³ School of Geosciences, University of Edinburgh, Edinburgh, United Kingdom

⁴ Central Natural Science Collections, Martin-Luther Universität Halle-Wittenberg, Halle, Germany

⁵ Department of Earth Sciences, University of Turin, Torino, Italy

Corresponding Author: Attila Ősi

Email address: hungaros@gmail.com

Based on associated and three-dimensionally preserved cranial and postcranial remains, a new thalattosuchian crocodyliform *Magyarosuchus fitosi* gen. et sp. nov. from the Lower Jurassic (Upper Toarcian) Kisgerecse Marl Formation, Gerecse Mountains, Hungary is described here. Phylogenetic analyses using three different datasets indicate that *M. fitosi* is the sister taxon of *Pelagosaurus typus* forming together the basal-most sub-clade of Metriorhynchoidea. With an estimated body length of 4.67–4.83 meter *M. fitosi* is the largest known non-metriorhynchid metriorhynchoid. Besides expanding Early Jurassic thalattosuchian diversity, the new specimen is of great importance since, unlike most contemporaneous estuarine, lagoonal or coastal thalattosuchians, it comes from an "ammonitico rosso" type pelagic deposit of the Mediterranean region of the Tethys. A distal caudal vertebra having an unusually elongate and dorsally projected neural spine reveals its strengthening role within a hypocercal tail fin that could have resulted in a slight ventral displacement of the distal caudal vertebral column in this basal metriorhynchoid. The combination of retaining heavy dorsal and ventral armors and having a slight hypocercal tail is unique, further highlighting the mosaic manner of marine adaptations in Metriorhynchoidea.

1 A NEW LARGE-BODIED THALATTOSUCHIAN CROCODYLIFORM FROM THE LOWER
2 JURASSIC (TOARCIAN) OF HUNGARY, WITH FURTHER EVIDENCE OF THE MOSAIC
3 ACQUISITION OF MARINE ADAPTATIONS IN METRIORHYNCHOIDEA

4

5

6 Attila Ósi,^{1,2,*} Mark T. Young,³ András Galács,¹ and Márton Rabi^{4,5}

7

8 ¹Eötvös University, Department of Paleontology, Pázmány Péter sétány 1/C, Budapest 1117,
9 Hungary, hungaros@gmail.com

10 ²Hungarian Natural History Museum, Ludovika tér 2, Budapest, 1083, Hungary

11 ³Grant Institute, School of Geosciences, The King's Buildings, University of Edinburgh, James
12 Hutton Road, Edinburgh, EH9 3FE, United Kingdom; marktyoung1984@gmail.com

13 ⁴Central Natural Science Collections, Martin-Luther University Halle-Wittenberg, Domplatz 4,
14 06108 Halle (Saale), Germany; iszkenderun@gmail.com

15 ⁵Department of Earth Sciences, University of Torino, Via Valperga Caluso 35, 10125, Torino,
16 Italy

17

18

19

20 *Corresponding author: Attila Ósi, hungaros@gmail.com

21

22

23 **Key words:** Crocodyliformes, Metriorhynchoidea, Toarcian, marine adaptation, Hungary

24

25 ABSTRACT

Based on associated and three-dimensionally preserved cranial and postcranial remains, a new thalattosuchian crocodyliform, *Magyarosuchus fitosi* gen. et sp. nov. from the Lower Jurassic (Upper Toarcian) Kisgrecse Marl Formation, Gerecse Mountains, Hungary is described here. Phylogenetic analyses using three different datasets indicate that *M. fitosi* is the sister taxon of *Pelagosaurus typus* forming together the basal-most sub-clade of Metriorhynchoidea. With an estimated body length of 4.67–4.83 meter *M. fitosi* is the largest known non-metriorhynchid metriorhynchoid. Besides expanding Early Jurassic thalattosuchian diversity, the new specimen is of great importance since, unlike most contemporaneous estuarine, lagoonal or coastal thalattosuchians, it comes from an "ammonitico rosso" type pelagic deposit of the Mediterranean region of the Tethys. A distal caudal vertebra having an unusually elongate and dorsally projected neural spine reveals its strengthening role within a hypocercal tail fin that could have resulted in a slight ventral displacement of the distal caudal vertebral column in this basal metriorhynchoid. The combination of retaining heavy dorsal and ventral armors and having a slight hypocercal tail is unique, further highlighting the mosaic manner of marine adaptations in Metriorhynchoidea.

INTRODUCTION

The Early Jurassic was a critical period in the initial development of marine adaptation in crocodylomorphs (Wilberg, 2015). Whereas the small-bodied, cursorial protosuchians existed on land (Colbert and Mook, 1951) and the nearshore to fluvial environments were inhabited by semi-aquatic goniopholidids (Tykoski et al., 2002), the first thalattosuchians appeared with the basal-most forms already showing a high number of anatomical traits suitable for a predominantly marine lifestyle (Young et al., 2010, Wilberg, 2015, Bronzati et al., 2015). Thalattosuchians are composed of two major groups, the teleosauroids and metriorhynchoids (Buffetaut, 1980; Young and Andrade, 2009; Young et al., 2010). Although teleosauroids were not as well-adapted to marine habitats as metriorhynchoids, their reduction in limb size and osteoderms (Buffetaut, 1980, 1982a; Young et al., 2016) coupled with a gracile and streamlined body, that had a relatively rigid skeleton capable of sub-undulatory swimming (Massare, 1988, Hua and Buffetaut, 1997), clearly shows that they were efficient swimmers. Metriorhynchoids, and especially metriorhynchids, on the other hand, became even more adapted to a marine lifestyle, evolving paddle-like limbs, hypocercal tail fin, enlarged preorbital salt glands, and osteoporotic-like bone tissues (Fraas, 1902, Andrews, 1913, Hua and Buffrénil, 1996, Young et al., 2010, Wilberg, 2015).

In the summer of 1996, a partial skeleton of a thalattosuchian crocodyliform from the Lower Jurassic Kisgeregse Marl Formation of northwestern Hungary was discovered (Kordos, 1998; Ósi et al., 2010). We present a detailed osteological work and a series of extensive phylogenetic analyses of this fossil and assign it to a new genus and species. Besides expanding Early Jurassic thalattosuchian diversity, the new specimen is of great interest since, unlike most contemporaneous estuarine, lagoonal or coastal thalattosuchians it comes from an "ammonitico rosso" type pelagic deposit.

This new taxon shows striking morphological similarities with the genus *Pelagosaurus*. However, the differences are enough to establish a new taxon, *Magyarosuchus fitosi* gen. et sp.

nov., based on autapomorphies and a unique combination of characters. Our three phylogenetic analyses support *Magyarosuchus fitosi* being the sister taxon to *Pelagosaurus*. However, the characters uniting these two taxa are unknown in other basal metriorhynchoids, and we cannot discount the possibility that they have a wider distribution, although they are absent in teleosauroids and metriorhynchids. The presence of *Magyarosuchus fitosi* in the Mediterranean Lower Jurassic increases the known range of morphological variation for basal metriorhynchoids. Not only is it the largest known non-metriorhynchid metriorhynchoid, but it has evidence of a slight ventral displacement of the distal caudal vertebral column. The combination of retaining dorsal and ventral osteoderms and having a slight hypocercal tail is unique, and further highlights the mosaic manner of marine adaptations in Metriorhynchoidea.

Institutional abbreviations—**BRLSI M**, Moore Collection of the, Bath Royal Literary and Scientific Institute, Bath, UK; **GPIT**, Paläontologische Sammlung der Eberhard Karls Universität Tübingen, Tübingen, Germany; **MTM**, Hungarian Natural History Museum, Budapest, Hungary; **NHMUK PV**, vertebrate palaeontology collection of the Natural History Museum, London, UK (OR, old register; R, reptiles); **SMNS**, Staatliches Museum für Naturkunde, Stuttgart, Baden-Württemberg, Germany; **UH, Urweltmuseum Hauff Holzmaden.**

GEOLOGICAL SETTING AND PALEOENVIRONMENT

Specimen was collected in one of the northwestern quarries of the Nagy-Pisznice Hill, close to Békás-Canyon (GPS coordinates: 47°42'09.4"N, 18°29'40.0"E), eastern Gerecse Mountains, northwestern Hungary (Fig. 1).

The remains of this large-bodied crocodyliform came from a fossiliferous limestone with a well-constrained stratigraphy (Galácz et al., 2010). These beds also yielded diagnostic ammonites, including *Grammoceras thouarsense* (d'Orbigny, 1844) which is an index fossil of the Upper

Toarcian (Lower Jurassic) *Grammoceras thouarsense* ammonite Zone. In lithostratigraphic terms, the bed yielding the vertebrate remains (Bed 13) corresponds to the uppermost section of the Kisgerecse Marl Formation (Fig. 2), a red, nodular clayey limestone widely distributed in the Gerecse Mountains (Császár et al., 1998). The overlaying beds belong to the Tölgyhát Limestone Formation, representing the uppermost Toarcian and the Aalenian-Bajocian in the Eastern Gerecse (Cresta and Galácz, 1990). The Kisgerecse Marl and the Tölgyhát Limestone Formations are members of the Jurassic calcareous sequence that is interrupted only by a few meters of siliceous radiolarite in the Middle Jurassic (Fodor and Főzy, 2013a; Fig. 2). The locality is in the eastern part of the Gerecse Mountains, which was a deeper, basinal area east to the Jurassic – Early Cretaceous submarine high (the ‘Gorba High’) in the western part of the mountains (see Vörös and Galácz, 1998).

The Jurassic of the Gerecse Mountains belongs to the Transdanubian Range of the Alpaca unit within the Alp-Carpathian framework (Fodor and Főzy, 2013b). The whole Jurassic sequence of the Gerecse is built up by pelagic carbonates which form a succession of reduced thickness and incomplete stratigraphic representation. This means that some stratigraphic units of subzonal or zonal rank may be missing in sections and these hiatus are indicated by so-called hard grounds, suggesting interruptions in sedimentation. All these phenomena are characteristic in these carbonate sequences of the Mediterranean region of the Mesozoic Tethys, where the dominant rocks are the so-called rosso ammonitico limestones and marls. These sequences are interpreted as deposited in the pelagic realm, on deeply submerged continental slope, far away from continental land masses, thus free of clastic material influx (see Bernoulli and Jenkyns, 2009). Pelagic environment with a comparatively deep-water depth is indicated also by the faunal composition of the ammonitico rosso type rocks: elements of benthic invertebrates are represented in insignificant amount (sporadic bivalves and brachiopods), and the single frequent group is of the nectonic cephalopods. The cephalopods, dominated by ammonoids, appear in

associations where the major groups are the phylloceratids and lytoceratids. These ammonite faunal compositions clearly indicate open marine environments with oceanic water depths with at least a few hundred meters (Westermann, 1990; Lukeneder, 2015).

MATERIAL, PRESERVATION AND METHODS

Material. The vertebrate material consists of a partial skeleton of a large-sized thalattosuchian crocodyliform including both cranial and postcranial remains. All the specimens are housed in the Vertebrate Collection of the Department of Paleontology and Geology of the Hungarian Natural History Museum (MTM). Unfortunately, detailed information on the circumstances of the fieldwork is not available. A very rough sketch of the specimen has been drawn during the work, but is not applicable for taking precise measurements.

Preservation. Since many Early Jurassic thalattosuchians (such as those of *Steneosaurus bollensis* and *Pelagosaurus typus*; e.g. Westphal, 1962) are known from flattened specimens preserved in laminated limestone, the three-dimensional preservation makes the new specimen particularly important. Furthermore, in many cases the finest details of skeletal anatomy, such as the shallow crest-like edges of the attachment surface of the cartilage on the epiphyses have been also preserved by the hard limestone matrix. On the other hand, due to the very slow sedimentation rate of these highly condensed Lower Jurassic rocks (Bernoulli and Jenkyns, 2009), some of the bone surfaces were partially dissolved, as seen for example, on the femoral mid-shafts. Dissolution of fossils from these strata, however, is not rare: ammonite shells are frequently found to have a complete lower side and a partially or completely dissolved upper side.

Methods. Specimens have been prepared both mechanically and chemically. Vibro-tool has been used for clearing the bones from the larger pieces of matrix. In some cases, chemical preparation using acetic acid was applied for a better cleaning of the bone surfaces.

150

151 The electronic version of this article in Portable Document Format (PDF) will represent a
 152 published work according to the International Commission on Zoological Nomenclature (ICZN),
 153 and hence the new names contained in the electronic version are effectively published under that
 154 Code from the electronic edition alone. This published work and the nomenclatural acts it
 155 contains have been registered in ZooBank, the online registration system for the ICZN. The
 156 ZooBank LSIDs (Life Science Identifiers) can be resolved and the associated information viewed
 157 through any standard web browser by appending the LSID to the prefix <http://zoobank.org/>. The
 158 LSID for this publication is: [urn:lsid:zoobank.org:pub:3623D096-C737-4B69-A491-
 159 ABC0F50FF4D4]. The online version of this work is archived and available from the following
 160 digital repositories: PeerJ, PubMed Central and CLOCKSS.

161

162 SYSTEMATIC PALEONTOLOGY

163

164 CROCODYLOMORPHA Hay, 1930 (*sensu* Nesbitt, 2011)
 165 THALATTOSUCHIA Fraas, 1901 (*sensu* Young and Andrade, 2009)
 166 METRIORHYNCHOIDEA Fitzinger, 1843 (*sensu* Young and Andrade, 2009)
 167 *MAGYAROSUCHUS* gen. nov.

168

169 urn:lsid:zoobank.org:act: [XXXXXX]

170

171 **Type species**—*Magyarosuchus fitosi* gen. et sp. nov. (type by monotypy).

172 **Etymology**—‘Hungarian crocodile’. *Magyaro* referring to the Hungarian people, and *suchus* is
 173 the Latinized form of the Greek *soukhos* (σοῦχος), meaning crocodile.

174 **Diagnosis**—Same as the only known species (monotypic genus).

MAGYAROSUCHUS FITOSI, gen. et sp. nov.

urn:lsid:zoobank.org:act: [XXXXXXX]

Holotype—middle third of left dentary (V.97.2A), posterior third of left dentary (V.97.2B), mandible fragment (V.97.2C), angular-surangular fragment (V.97.40); 21 teeth (V.97.1., V.97.4., V.97.53., V.97.5., V.97.24., V.97.37., V.97.29., V.97.55., V.97.56.); three dorsal vertebrae (V.97.26., V.97.30.); two sacral vertebrae (V.97.30.); two proximal caudal vertebrae (V.97.29., V.97.30.); six mid-caudal vertebrae (V.97.27. V.97.28.); twelve distal caudal vertebrae (V.97.19., V.97.21., V.97.22., V.97.27., V.97.31.); twenty-eight dorsal rib fragments (V.97.16., V.97.14., V.97.46., V.97.15., V.97.8., V.97.17., V.97.47., V.97.67., V.97.51., V.97.52., V.97.54., V.97.64., V.97.68, V.97.48., V.97.38); sacral ribs (V.97.37., V.97.27.); coracoideum (V.97.7.); radius (V.97.42.); right ilium (V.97.44.); left ilium (V.97.34.); left ischium (V.97.36.); left pubis (V.97.49.); right pubis (V.97.35.); left femur (V.97.13.), right femur (V.97.33.); right tibia (V.97.9.); left tibia (V.97.69.); fibulae? (V.97.41., V.97.43.); four metapodial elements (V.97.10., V.97.11., V.97.38., V.97.45.); phalanges (V.97.61.); other limb bones (V.97.15.); four dorsal osteoderms (V.97.59., V.97.60); twelve ventral osteoderms (V.97.18., V.97.38, V.97.65.); twenty-seven fragmentary osteoderms (V.97.4., V.97.53., V.97.24., V.97.60., V.97.56.); other fragmentary elements: V.97.49., V.97.50., V.97.58., V.97.60.). Note that in some cases, the same catalogue number belongs to different bones or teeth because blocks of rock contain more than one element and these blocks have been assigned to catalogue numbers. Measurements of the bones are listed in Table 1.

Etymology—‘Fitos’s Hungarian crocodile’. The name refers to Attila Fitos, discoverer of the specimen for thanking his donation of the fossil to science.

Type locality— one of the northwestern quarries of the Nagy-Pisznice Hill, close to Békás-canyon (GPS coordinates: 47°42'09.4"N, 18°29'40.0"E), eastern Gerecse Mountains, northwestern Hungary.

Type horizon—Bed 13, Kisgercse Marl Formation, Transdanubian Central Range. *Grammoceras striatulum* ammonite Subzone, *Grammoceras thouarsense* ammonite Zone, upper Toarcian, Lower Jurassic (Galácz et al., 2010).

Diagnosis—Metriorhynchoid thalattosuchian with the following unique combination of characters [proposed autapomorphic characters are indicated by an asterisk (*): large body size (estimated body length: in the range of 4.67–4.83 m); tooth crown carinae development variable, being well-developed apically, beginning to develop mid-crown and absent in the basal region; enamel ornamentation is composed of ridges that differ in arrangement on the labial and lingual surfaces, being more widely spaced on the labial surface than the lingual surface, with the lingual surface having tightly packed apicobasal ridges basally which apically become shorter and discontinuous, and the apical lingual ridges on the mesial and distal margins bend towards the carinae (but do not contact them)*; abrupt change in centrum shape of the distal caudal vertebrae, with strong mediolateral compression (i.e. distal vertebrae are clearly heteromorphic); dorsal osteoderms have irregularly shaped pits (including circular, ellipsoid, bean-shaped, triangular and quadrangular shapes), with an extreme variation in size (from small to very large), with elongate pits present on the ventrolateral surface running from the keel to the lateral margin*; dorsal osteoderms have an anterolateral process that is ‘indistinct, no longer being distinctly ‘peg-like’, as their lateral margin is contiguous with that of the osteoderm ventrolateral surface*.

Characteristics shared with Pelagosaurus. *Magyarosuchus fitosi* shares the following two synapomorphies with *Pelagosaurus*: (1) the surangulodentary and angulodentary grooves are parallel and positioned close to one another ventral to the dentary rami tooth row; and (2) the presence of a distinct anterior acetabular flange on the ilium, created by the anterior acetabular

margin projecting anteriorly such that it is anterior to the iliac anterior margin. However, these two characters are currently unknown in all other basal metriorhynchoids and their distribution is therefore unknown. However, they are absent in teleosauroids and metriorhynchids (e.g. Fraas, 1902; Andrews, 1913; Johnson et al., 2017).

Metriorhynchoid characteristics shared. Magyarosuchus fitosi has the following two metriorhynchoid synapomorphies: (1) a coracoid with both the proximal and distal ends convex, and (2) the femur posteromedial tuber is present and the largest of the proximal tubera.

DESCRIPTION AND COMPARISONS

Cranial elements

Mandible. Three fragments (MTM V.97.2.) of the left mandible are preserved. Based on the mandibular proportions of *Pelagosaurus typus* (BRLSI M1413, Pierce and Benton, 2006) the first fragment (MTM V.97.2.A, Fig. 3A-B) most probably represents the middle third of the dentulous part of the dentary. There is no indication of any post-dentary bones preserved on this element. It has a dorsoventrally high profile. The ventral side is eroded and the medial side is covered with hard matrix, thus it is not clear whether this part formed already the symphyseal region. Laterally, it possesses two anteroposteriorly extending grooves parallel with each other, a feature that is also present in *Pe. typus* (BRLSI M1413, MTM M 62 2516). On the dorsal or laterodorsal side of the bone, six large (diameter: 10 mm) alveoli can be observed. They have an oblique, anterolabial-posterolingual orientation suggesting that the teeth oriented anterolabially or slightly dorsolabially instead of pointing simply dorsally. Inter-alveolar septa are anteroposteriorly thick (ca. 7-10 mm) reflecting widely spaced teeth in this part of the tooth row. Some pits as part of the lateral ornamentation can be observed, but it is not clear how developed this ornamentation was on the lateral side since this surface has been slightly dissolved due to diagenetic processes.

The second fragment (MTM V.97.2.B, Fig. 3C-E) is the posterodorsal segment of the left dentary. Although there is no direct connection preserved with the dentary fragment described above, this second piece is apparently the posterior continuation of that element. Anterodorsally, it bears the last three alveoli which show a similar orientation and widely spaced configuration as those seen on the first fragment. Posterior to the last alveolus, the dentary becomes slightly elevated to form the shallow lateral side of the coronoid process. Medially, the anterodorsal part of the deeply concave mandibular adductor fossa can be observed. The ventral side of the specimen is missing (Fig. 3E). The lateral surface is generally smooth, but on the ventral part some pits as part of the sculpture are present. In *Pe. typus* (BRLSI M1413) this part of the mandible was formed by the surangular and the dentary (Pierce and Benton, 2006, MTM M 62 2516, pers. obs.). However, in *Magyarosuchus fitosi* the dentary-surangular suture cannot be detected. On the dorsal side, posterior to the last alveolus a shelf is present that has a slightly elevating medial side.

The third block (MTM V.97.40., Fig. 3F-I) preserved from the left mandible represents the dorsal and ventral margins of the mandibular fenestra. The dorsal part is the middle portion of the surangular and the posterior process of the dentary and the ventral piece is the middle portion of the angular. On the dorsal piece, the dentary-surangular suture is observable. The lateral surface of the bones is smooth being completely avoid of the pitted ornamentation. Medially, they are concave forming the dorsal, lateral and ventral margins of the mandibular adductor fossa. Ventrally, the angular is widened forming a massive ventral bar of the postdentary part of the mandible. On its posteroventral surface, some grooves can be observed which, according to Iordansky (1973) and Mueller-Töwe (2006), should have served as the insertion of *Musculus pterygoideus posterior*.

A fourth element (MTM V.97.2.C; Fig. 3J-L) is probably from the right post-dentary part of the mandible. It is too fragmentary to tell more details on it position.

Teeth. Twenty-one teeth or tooth fragments have been preserved associated with the skeleton. These have conical and generally massive crowns (Fig. 4) being much more robust than the teeth of *Pelagosaurus*. They have a circular or sub-circular cross-section and some teeth are quite elongated with a crown height/width ratio over three (Fig. 4A, B), whereas others are stockier with a ratio of two or less (Fig. 4C-F). In contrast to *Pe. typus* (MTM M 62 2516) but similar to *Zoneait nargorum* (Wilberg, 2015), all teeth bear mesial and distal unserrated carinae which disappear towards the base of the crown (Fig. 4E-I). Crown surface is ornamented by longitudinal enamel wrinkles on all sides (Fig. 4H-I) that are more prominent than those in *Steneosaurus bollensis* (MTM M 69 242). Morphology of the posterior teeth are generally similar to those of *Lemmysuchus obtusidens* (Johnson et al., 2017), but they are devoid of any type of serration and enamel wrinkles apically are not anastomosing as in the latter taxon. Roots are preserved in most of the teeth and are two to three times longer than the crowns, and together with the crowns they are strongly curved lingually (Fig. 4C-F). Wear pattern due to tooth-tooth contact cannot be observed on the tooth crowns.

Post-cranial axial skeleton

The vertebral column is not complete, represented only by three dorsal, two sacral, and 20 caudal vertebrae. All the vertebrae are platy- or slightly amphicoelous, and are devoid of pneumatic foramina. Neural arches are fully fused to the centra in all elements. Cervical vertebrae seem to be not preserved in the material.

Dorsal vertebrae. The centrum of dorsal vertebrae (MTM V.97.26., MTM V.97.30) is higher than wide, moderately concave laterally and ventrally (Fig. 5A-C). Its ventral surface is devoid of any grooves or crests. Anterior and posterior articulation surfaces are oval to slightly trapezoid in shape. Transverse processes emerge from the lateral side of the neural arch. The neural spine is rectangular in lateral view and its height is approximately three-fourth of that of the centrum.

Sacral vertebrae. Sacral vertebrae (MTM V.97.30.) are preserved in a complex with the last lumbar and the first caudal vertebrae (Fig. 5D-E). There are two true sacral vertebrae, as is the norm for thalattosuchians (e.g. Fraas, 1902; Andrews, 1913; Westphal, 1962), and in contrast to machimosaurin teleosauroids which have three due to the sacralisation of the first caudal vertebra (Andrews, 1913; Hua, 1999; Young et al., 2014; Johnson et al., 2017). Since a thin layer of sediment can be observed between the vertebrae, they were supposedly not co-ossified. The two sacral vertebrae are quite similar to each other in having lateromedially wide and ventrally concave centra. Sacral ribs are not fused to the centra in contrast to the condition seen in *Steneosaurus bollensis* (MTM M 69 242). Their articulation surface on the centra are large, anteroposteriorly elongated, oval shaped surfaces among which those of the anterior sacral are in an anterior and those of the posterior are in a posterior position. Whereas the neural arches seem to be fused, the neural spines are separated, short processes.

Caudal vertebrae. The first caudal, being fused to the second sacral (MTM V.97.30., Fig. 5D-E), is longer than wide and as wide as high being ventrally very slightly concave, and the broken transverse processes are in an anterior position on the side of the centrum. The neural spine is shallow, having ca. half of the height of the centrum. The more posterior caudal vertebrae are more elongate and lateromedially slightly compressed with moderately concave lateral and ventral sides (Fig. 5F-G). Articular surfaces are oval in the mid-series caudal vertebrae, whereas they are rounded or slightly rectangular in the distal caudals. Transverse processes are positioned close to the centrum-neural arch fusion and posteriorly they become gradually shorter, laterally projecting processes. Similar to the 11th to the 22nd caudal vertebrae of *Pelagosaurus typus* (MTM M 62 2516), the neural spines of two of the preserved caudals of *Magyarosuchus fitosi* (MTM V.97.31) are divided into a smaller, triangular, dorsally or anterodorsally projecting process and a larger, posterodorsally oriented process (Fig. 5H-J).

The distal-most preserved caudal (MTM V.97.19., Fig. 5K-P) is the posterior half or two-third of the complete vertebra. Here, the neural spine is an anteroposteriorly wide, relatively massive, plate-like element. Its preserved part is as high as the centrum but is broken both anteriorly (Fig. 5N) and dorsally (Fig. 5O) indicating that it was originally much higher. In *Pe. typus* (MTM M 62 2516) and *Steneosaurus bollensis* (MTM M 69 242), the distal caudals have only a posterodorsally projecting, anteroposteriorly narrow spine that emerges only on the posterior half of the centrum. The posterior articular surface of the centrum is close to quadrangular in shape and slightly concave.

Ribs. Numerous fragmentary ribs and rib fragments are preserved and they are generally similar to those of extant crocodylians. Two of them are interpreted as dorsal ribs in having an elongate, anteroposteriorly wide capitulum and a relatively short tuberculum. In cross-section they are close to oval shaped, but they bear a shallow crest on the posterior side of their proximal half that disappears distally.

Three of the sacral ribs are preserved (Fig. 6C-F). All of them are short and massive with oval shaped (in MTM V.97.37. slightly rugose) articular surface. In anteroposterior view, they are triangular in shape with a slightly lateroventrally bent distal end. MTM V. 97.37 is the largest, has a convex crest-like dorsal margin and probably represents the first sacral rib. The third specimen (97.27) is strongly eroded but the vertebral articulation is partly preserved.

Appendicular skeleton

Coracoid. From the pectoral girdle elements only the right coracoid (MTM V.97.7.) is preserved in two pieces (Fig. 6G-H). It has the same bow-tie morphology as that of *Pelagosaurus typus* (Pierce and Benton, 2006) and *Steneosaurus bollensis* (Westphal, 1962) with concave anterior and posterior margins and a convex ventral articulation surface. The medial surface is concave and partly resorbed due to diagenetic processes, whereas the lateral surface is smooth with a

marked, oval-shaped coracoid foramen piercing it. The glenoid is a slightly convex surface. The distal half is strongly flattened and divergent ending dorsally in a convex edge.

Radius. From the forelimbs, only the proximal end of one radius (MTM V.97.42.) is preserved (Fig. 7A-B). The radius slightly widens towards the articular region and has a concave articular surface being similar to that of *Steneosaurus bollensis* (MTM M 69 242) and *Platysuchus multiscrobiculatus* (SMNS 9930, Westphal, 1962).

Ilium. Both ilia (MTM V.97.34., MTM V.97.44.) are preserved (Fig. 6I-M). The left one (MTM V.97.34) is more complete and only its medial side with the articulation of the sacral ribs is covered with sediment (Fig. 6I-L). In general, the ilium is very similar to that of *Steneosaurus bollensis* (MTM M 69 242) and *Pelagosaurus typus* (MTM M 62 2516) in having a rhomboidal form in lateral view with a large circular and deep acetabulum. Posteroventrally, its articulation surface for the ischium is not straight as in *S. bollensis* but slightly concave as that of *Pe. typus*. Dorsally, a massive and straight iliac crest is present with a pointed anterior process reaching the anterior, crested margin of the acetabulum. This process is relatively more developed than that of *Lemmingsuchus obtusidens* (Johnson et al., 2017). Posteriorly, the iliac crest ends in a massive triangular boss with a slightly convex posteroventral edge as in *Pe. typus*. The pubic process of the ilium can be observed only from the medial side of the right ilium that is a ventrally projected massive process, but the articulation surface is not preserved.

Ischium. Only the distal half of the left ischium (MTM V.97.36) is preserved. It is a bard-shaped element with developed, radially oriented, elongate grooves and shallow crests on its lateral surface for muscle attachments (Fig. 6P). Whereas its ventral edge is slightly convex, the posterodorsal one is slightly concave. Its anterior process is broken. The posterior process is strongly pointed similar to that of *Pelagosaurus typus* (BSGP 1890 I 509/11, MTM M 62 2516) or *Steneosaurus bollensis* (UH 13, Mueller-Töwe, 2006).

Pubis. Both pubes are preserved. From the right one (MTM V.97.49.) is only the distal half preserved, whereas the left one (MTM V.97.35.) is complete (Fig. 6N-O) but can only be studied in lateral view. It is an elongate, rod-like element with slightly widened proximal end having an oval shaped, articular surface. Whereas the posteroventral margin is almost straight, in contrast to that of *Platysuchus multiscrobiculatus* (SMNS 9930, Westphal, 1962), the anterodorsal one is slightly concave resulting in a widened distal end. The lateral surface of the distal end is ornamented by radial grooves for muscle attachments. The pubis of *Magyarosuchus fitosi* differs from that of *Pelagosaurus typus* (MTM M 62 2516) in having a marked upward bending of the distal end and from that of *Steneosaurus bollensis* where it bends rather downward (Mueller-Töwe, 2006). It also differs from the pubis of *Pl. multiscrobiculatus* in having a strongly convex distal margin.

Femur. Both femora (MTM V.97.13. left, MTM V.97.33. right) are complete but their shafts are broken and slightly dissolved due to diagenetic events (Fig. 7D-I). In general, the femur of *Magyarosuchus fitosi* shows the typical crocodylomorph conservative shape with the shaft bending anteriorly and the proximal third of the bone curving slightly medially. The proximal end has a smooth, rounded articulation surface with dorsomedially oriented femoral head (Fig. 7H). The fourth trochanter cannot be observed. The distal end has well developed, rounded medial and lateral condyles bordering a marked intercondylar groove. The femur of *M. fitosi* is very similar to that of *Steneosaurus bollensis*, *Platysuchus multiscrobiculatus* or *Pelagosaurus typus*, but *Pl. multiscrobiculatus* has proportionally slightly shorter femur (Westphal, 1962; Mueller-Töwe, 2006).

Tibia. Both tibiae (MTM V.97.9., MTM V.97.69.) are preserved and complete with the left one (MTM V.97.9.) being intact (Fig. 7J-O). It is a straight, slightly anteriorly bowing element with moderately widened proximal and distal ends as seen in *Pelagosaurus typus* (MTM M 62 2516) and *Steneosaurus bollensis* (Westphal, 1962; Mueller-Töwe, 2006). It clearly differs from the

tibia of *Lemmysuchus obtusidens* in having a more gracile shaft (Johnson et al., 2017). Planes of proximal and distal ends have an angle of approximately 135° as typically seen in sauropsid tibiae. The proximal end shows two flat to very slightly concave platforms to accept the distal condyles of the femur. The cnemial crest is wide and massive projecting anteriorly. The distal end is oval shaped and slightly rounded (Fig. 7O). The length of the tibia (210 mm) is 58% of the femur length (360 mm). This proportion is more similar to that of *Steneosaurus bollensis* (MTM M 69 242: 59%, MTM uncatalogued 1: 56%, MTM uncatalogued 2: 58%) and *Platysuchus multiscrobiculatus* (SMNS 9930: 60% Mueller-Töwe, 2006) than that of *Pelagosaurus typus* (MTM M 62 2516: 50%) or *Lemmysuchus obtusidens* (NHMUK PV R 3168: ~50%).

Fibula. The two proximal halves (MTM V.97.15., MTM V.97.41., Fig. 7P-R) and one of the distal parts (MTM V.97.43., Fig. 7S-T) of the fibulae are preserved. The proximal end is slightly divergent proximally and bowed in the anteroposterior plane. The proximal articular surface is oval shaped, and slightly convex. The distal end is straight and less divergent distally than the proximal end. The distal articular surface is convex and slightly obliquely oriented relative to the longitudinal axis of the bone. The preserved parts of the fibulae of *Magyarosuchus fitosi* are similar to those of *Steneosaurus bollensis* and *Pelagosaurus typus* (Mueller-Töwe, 2006).

Astragalus. The left astragalus (MTM V.97.12.) is one of the best preserved elements of the skeleton showing all articulation surfaces (Fig. 8A-F). It is a cubic element as typically seen in archosauromorphs (Schaeffer, 1941; Parrish, 1987; Sereno and Arcucci, 1990). The dorsomedially positioned tibial articular surface is anteroposteriorly as long as mediolaterally and has a concave surface. The fibular articulation is a short block, being not as elongated as that of *Simosuchus clarki* (Sertich and Groenke, 2010), and the articulation surface is a well developed, tetragonal and concave surface as seen in e.g. *Proterosuchus* species or in extant crocodylians (Cruickshank, 1979; Parrish, 1987; Sereno and Arcucci, 1990). Dorsally the tibial and fibular articulation surfaces are separated by an anteroposteriorly short but well developed crest.

Anteroventrally, the slightly convex surface is present for the metatarsal I. In posterior view, ventral to the fibular articulation, a deep groove extends lateromedially separating the dorsal part from the ventral, astragalar trochlea. This groove continues medioventrally and contains two small nutritive foramina. The astragalar trochlea ends laterally in the calcaneal peg that fitted in the socket-like articular surface of the calcaneum. This morphology indicates a 'crocodile-normal' ('CN' of Chatterjee, 1978) crurotarsal ankle type in *M. fitosi*, similar to that of *Steneosaurus bollensis*, *Pelagosaurus typus* and *Platysuchus multiscrobiculatus* (Westphal, 1962; Mueller-Töwe, 2006). Articulation surfaces and tendon attachment areas appear to be more complex in *M. fitosi* than in *Lemmingsuchus obtusidens* (Johnson et al., 2017). The astragali of metriorhynchids are even less complex, being mediolaterally compressed and rounded (Fraas, 1902; Andrews, 1913). The astragalus of *M. fitosi* was obviously freely movable relative to the tibia in contrast to that of *Orthosuchus* species (Nash, 1968).

Metapodium. Three of the metatarsals (MTM V.97.10., MTM V.97.11., MTM V.97.45.) are preserved. Based on the length/width proportions compared to *Steneosaurus bollensis* (MTM M 69 242) and *Pelagosaurus typus* (MTM M 62 2516), one of them (MTM V.97.10) represents one of the third metatarsals (Fig. 8G-J). The second one (MTM V.97.11.) is the two-third of the second or third metatarsals. They show the same morphology as the second and third metatarsals of basal thalattosuchians (Delfino and Dal Sasso, 2006; Mueller-Töwe, 2006), in having a long, straight shaft, oval to slightly rectangular cross-section, and a slightly widened distal articular end. Distal condyles are moderately developed and separated by a shallow intercondylar groove. The third specimen (MTM 97.45.) is too fragmentary to determine its more precise position.

Phalanges. A single phalanx (MTM V.97.61.) is preserved (Fig. 8K-L). It is two times longer than wide and has an hour-glass shape. Articular surfaces are poorly preserved. Compared to the phalanges of *Steneosaurus bollensis* or *Platysuchus multiscrobiculatus* (Westphal, 1962; Mueller-Töwe, 2006), it is most similar to the first phalanx of the first manual digit of these taxa.

Unidentified limb bones. The material consists of two fragmentary limb bones. One element might represent one of the metacarpals or the ulnare (MTM V.97.38, Fig. 6C) in having a robust shaft and massive articulations proximally and distally. The other element is perhaps the distal end of the other fibula (Fig. 8S-T).

Dermal ossifications

Forty-three dorsal and ventral osteoderms are preserved. Many of these (MTM V.97.4., MTM V.97.24., MTM V.97.53., MTM V.97.56.) are still in matrix and only a small piece or the cross-section of them can be observed thus their position is unknown. Nevertheless, osteoderm morphology differs from those of other thalattosuchians and diagnoses *Magyarosuchus fitosi*.

Dorsal armor. Four osteoderms (MTM V.97.59., MTM V.97.60.) can be certainly referred to the dorsal armor. They are large rectangular to slightly rounded elements with an anteroposteriorly extending dorsal keel dividing the osteoderm into a greater medial and a smaller lateral part (Fig. 9A-F). The anterior margin of the osteoderms is smooth and oblique to overlap the posterior surface of the anteriorly following osteoderm. Whereas two dorsal osteoderms are flat or very slightly concave ventrally (Fig. 9A-D), the two others are strongly bent dorsally (Fig. 9E-F). More prominent in these strongly bent osteoderms, but also present in the case of the two other dorsal osteoderms, is the anteroposterior keel that extends into a well-developed triangular anterolateral process (Fig. 9A, D, E). This anterolateral process is present in all basal thalattosuchians, including *Pelagosaurus typus* (as the mid-posterior dorsal osteoderms, which are typically in articulation, bear this process; MNHN.F RJN 463), but in these taxa it is more pronounced having a quite angular medial margin (Westphal, 1962) in contrast to that of *Magyarosuchus fitosi*. The shape of this process in *M. fitosi* is more reminiscent of the mid-posterior dorsal osteoderms of the Middle Jurassic teleosauroids *Lemmingsuchus obtusidens* and *Steneosaurus edwardsi* (Andrews, 1913; Adams-Tresman, 1987; Johnson et al., 2017).

Ornamentation is also unique in *M. fitosi*. Dorsal surface is ornamented by the proportionally largest pits among thalattosuchians, thus the margin between the pits is frequently very thin. Pits are usually not circular but oval, triangular or rhomboidal in shape.

Ventral armor. Twelve elements (MTM V.97.38.) can be referred to the ventral armor. Some of them form complex, fused blocks (Fig. 9G-I). The largest among these contains six fragmentary osteoderms (Fig. 9G). Ventral osteoderms are lateromedially wider than their anteroposterior length. Anteriorly they bear a smooth, oblique surface for the articulation of the overlapping anterior element, as seen on the dorsal osteoderms. They are devoid of any processes on their margins and dorsally they do not bear crests. Their ventral surface is ornamented by large pits morphologically similar to those of the dorsal osteoderms.

PHYLOGENETIC ANALYSIS

Methods

Three phylogenetic analyses were conducted to assess the evolutionary relationships of *Magyarosuchus fitosi* gen. et sp. nov. within Thalattosuchia. The character scoring for *M. fitosi* was based on first-hand examination of the holotype by MTY, MR and AÖ. Three datasets were employed to conduct these analyses, two of which were first presented in Ristevski et al. (2018) and are also in an ‘in review’ manuscript. However, both of these datasets have been extensively updated herein as they form the basis of the ongoing Crocodylomorph SuperMatrix Project. The first dataset is a merged matrix combining the two datasets originally published by Young et al. (2016), which was then subsequently revised and expanded, hereafter we refer to it as the Hastings + Young matrix (or H+Y matrix); whilst the second is an updated and expanded version of the dataset originally by Andrade et al. (2011), hereafter referred to as the modified Andrade matrix (or mA matrix). The third and final dataset used herein is that of Wilberg (2017). All data are summarized in Supplementary data files DataS1-S6.

The first parsimony analysis presented here employs the H+Y matrix. The two parent matrices for the H+Y matrix were presented in Young et al. (2016): dataset 1 (the Hastings matrix), contained 37 operational taxonomic units (OTUs) scored for 120 morphological characters; whilst dataset 2 (the Young matrix), contained 103 OTUs scored for 298 characters. Mark Young, Alexander Hastings and Thomas Smith merged the matrices in 2016-2017. This resulted in extensive re-examination of all characters, re-scoring of characters to ensure a common and agreed philosophical approach to character construction, ensuring the OTUs from both datasets were scored for all characters, and the addition of characters from Andrade et al. (2011) and Nesbitt (2011). Some OTUs were revised and new ones added (see Ristevski et al., 2018 and Smith et al. in review for full details). This resulted in the current iteration of the H+Y matrix containing a total of 140 OTUs scored for 454 characters. Excluding *M. fitosi*, seven of the 140 OTUs are basal metriorhynchoids, forty-two are metriorhynchids, and eighteen are teleosauroids. 25 characters representing morphoclines were treated as ordered (7, 28, 36, 49, 57, 98, 164, 166, 174, 205, 225, 228, 234, 264, 274, 330, 357, 362, 372, 407, 410, 420, 421, 423, 435). For the H+Y matrix, *Postosuchus kirkpatricki* Chatterjee, 1985 was used as the outgroup taxon.

The second parsimony analysis presented here employs the mA matrix: a modified version of the character and taxon list first published by Andrade et al. (2011), which originally included 104 OTUs scored for 486 characters. As per the recommendations of Andrade et al. (2011), Halliday et al. (2013), and Puértolas-Pascual et al. (2015), the putative goniopholidid *Denazinosuchus kirtlandicus* (Lucas and Sullivan, 2003), and the Asian taxon “*Goniopholis*” *phuwiangensis* Buffetaut and Ingavat, 1983 OTUs, along with the composite “*G.*” *phuwiangensis* + *Siamosuchus* terminal (ALTSiamosuchus), were excluded due to their instability and, in the case of the latter, inapplicability. Following Halliday et al. (2013) and Ristevski et al. (2018) the putative goniopholidids *Kansajasuchus extensus* Efimov, 1975, *Sunosuchus shartegensis* Efimov,

1988 and *Turanosuchus aralensis* Efimov, 1988 were excluded due to their instability. In total, the analysis of the mA matrix presented here included 110 OTUs scored for 570 characters. Excluding *M. fitosi*, one of the 110 OTUs are basal metriorhynchoids, ten are metriorhynchids, and three are teleosauroids. 31 characters representing morphoclines were treated as ordered (6, 9, 32, 71, 72, 125, 146, 153, 158, 216, 218, 222, 245, 271, 297, 302, 303, 326, 355, 378, 379, 446, 467, 471, 481, 523, 526, 536, 537, 539, 551). For the mA matrix, *Gracilisuchus stipanicorum* Romer, 1972 was the outgroup taxon.

For both the H+Y and mA datasets the primary differences between our analyses and those presented by Ristevski et al. (2018) are: (1) the continued merging of the two datasets as part of the Crocodylomorph SuperMatrix Project, which has been the primary cause of the general increase in character number of both datasets; (2) the addition of *M. fitosi* into both datasets; (3) revision of current characters based on those from Nesbitt (2011), Narváez et al. (2015), Buscalioni (2017), Leardi et al. (2017) and Nesbitt and Desojo (2017), and the addition of new ones from those papers; and (4) the creation of new characters to help explore some morphofunctional complexes (such as the hypocercal tail in metriorhynchoids).

The Wilberg dataset (hereafter W matrix), is largely the same as that presented in Wilberg (2017). The only differences are: (1) the addition of *M. fitosi*; (2) the addition of two characters from the two merged datasets (the mandibular parallel grooves character and the flange-like ilium anterior margin character); and (3) some minor rescoring of teleosauroids based on personal observations by MTY (see Online Supplementary). This resulted in the current iteration of the W matrix containing a total of 98 OTUs scored for 408 characters. Excluding *M. fitosi*, five of the 98 OTUs are basal metriorhynchoids, twelve are metriorhynchids, and ten are teleosauroids. 40 characters representing morphoclines were treated as ordered (26, 51, 58, 59, 61, 64, 83, 128, 148, 151, 163, 202, 203, 208, 210, 220, 224, 240, 255, 261, 263, 265, 270, 296, 304, 311, 316,

342, 344, 345, 346, 362, 366, 373, 375, 384, 386, 393, 394, 399). For the W matrix,
Gracilisuchus stipanicorum was used as the outgroup taxon.

The cladistic analyses were conducted following the methodology implemented by Young
et al. (2016), using TNT v1.5, Willi Hennig Society Edition (Goloboff and Catalano, 2016).
 Memory settings were increased with General RAM set to 900 Mb and the maximum number of
 trees to be held set to 99,999. In the analysis of each matrix, cladogram space was searched using
 the advanced search methods in TNT (sectorial search, ratchet, drift and tree fusion) for 1000
 random addition replicates. The default settings of the advanced search methods were modified to
 increase the number of iterations of each method per analysis replicate (except for tree fusion,
 which was kept at 3 rounds). For the sectorial search, 1000 drifting cycles were applied for
 selections of above 75 with 1000 starts, and trees were fused 1000 times for those below 75. TNT
 also conducted 1000 rounds of consensus sectorial searches (CSS) and 1000 rounds of exclusive
 sectorial searches (XSS). The analysis included 1000 ratchet iterations with the cease
 perturbation phase reached when 1000 substitutions were made or 99% of swapping was
 completed. The program incorporated 1000 drift cycles within the analysis, which also reached
 the cease perturbation phase at 1000 substitutions made or 99% of swapping completed.

Results

The first phylogenetic analysis that utilised the H+Y matrix recovered 84 most-parsimonious
 cladograms (MPCs) with 1477 steps (ensemble consistency index, CI = 0.417; ensemble
 retention index RI = 0.842; rescaled consistency index RC = 0.351; ensemble homoplasy index
 HI = 0.583). Overall, the strict consensus topology recovered from this analysis (Fig. 10A) is
 very similar to the ones presented in Ristevski et al. (2018) and *Smith et al. (in review)*. The only
 difference within Thalattosuchia is the addition of *Magyarosuchus fitosi*, which is found to be the

sister taxon of *Pelagosaurus typus* (Fig. 10A). The overall picture of crocodylomorph interrelationships found herein are the same as those found in previous iterations of this merged dataset (Ristevski et al., 2018; [Smith et al. in review](#)): the rauisuchian *Postosuchus kirkpatricki* lies outside the clade that unites all other taxa (i.e. Crocodylomorpha), with ‘sphenosuchians’ forming a grade of more derived taxa. Protosuchidae and the shartegosuchid *Fruitachampsia callisoni* Clark, 2011 are recovered as basal crocodyliforms. The remaining taxa comprise Mesoeucrocodylia, which includes a clade formed by *Eopneumatosuchus colberti* Crompton and Smith, 1980 + Thalattosuchia, and the other clade being Metasuchia. Metasuchia contains two sub-clades, Notosuchia and Neosuchia. Within Thalattosuchia, both [Teleosauroidea](#) and Metriorhynchoidea are recovered as monophyletic. *Pelagosaurus typus* is found to be a basal metriorhynchoid, and Metriorhynchidae, Metriorhynchinae, Rhacheosaurini, Geosaurinae and Geosaurini are all found to be monophyletic (Fig. 10A).

The second phylogenetic analysis that utilised the mA matrix yielded 16 MPCs with 2472 steps (CI = 0.305; RI = 0.764; RC = 0.233; HI = 0.695). Overall, the strict consensus topology recovered from this analysis is very similar to the ones presented in Ristevski et al. (2018) and [Smith et al. \(in review\)](#). The only differences within Thalattosuchia are: (1) the addition of *M. fitosi*, which is found to be the sister taxon of *Pe. typus*; (2) teleosauroids are no longer in a polytomy, but now *Steneosaurus bollensis* is the sister taxon to a clade *S. heberti* + *Platysuchus multiscrobiculatus*; and (3) *Metriorhynchus superciliosus* is no longer the sister taxon to Geosaurini (but in a trichotomy with Geosaurini and Rhacheosaurini) (Fig. 10B). The overall picture of crocodylomorph interrelationships found herein are the same as those found in previous iterations of this dataset: gracilisuchid *Gracilisuchus stipanicorum* lies outside the clade that unites all other taxa (i.e. Crocodylomorpha), with ‘sphenosuchians’ forming a grade of more derived taxa. Protosuchidae, *Gobiosuchus* and *Hsisosuchus* are recovered as successively more derived basal crocodyliforms. The remaining taxa comprise Mesoeucrocodylia, which

contains two sub-clades, Notosuchia and Neosuchia. Thalattosuchia is recovered within Neosuchia, as the sister taxon to Tethysuchia. Within Thalattosuchia, both Teleosauroidea and Metriorhynchoidea are recovered as monophyletic. *Pelagosaurus typus* is found to be a basal metriorhynchoid, and Metriorhynchidae, Rhacheosaurini and Geosaurini are all found to be monophyletic (Fig. 10B).

The final phylogenetic analysis, utilising the W matrix, recovered six MPCs with 1777 steps (CI = 0.306; RI = 0.733; RC = 0.224; HI = 0.694). The strict consensus topology recovered from this analysis is almost identical to the analysis by Wilberg (2017), the only difference is the addition of *M. fitosi* (which is found to be the sister taxon of *Pe. typus*). The overall picture of crocodylomorph interrelationships found herein are the same as that found in Wilberg (2017): the gracilisuchid *Gracilisuchus stipanicorum* and rauisuchian *Postosuchus kirkpatricki* lies outside the clade that unites all other taxa (i.e. Crocodylomorpha), with ‘sphenosuchians’ forming a grade of more derived taxa. Thalattosuchians are found to be the sister taxon to Crocodyliformes (Fig. 11). Within Crocodyliformes there are two sub-clades: Mesoeucrocodylia, and one formed by Protosuchidae, Shartegosuchidae, Gobiosuchidae and *Hsiosuchus*. The remaining taxa comprise Mesoeucrocodylia, which contains two sub-clades, Notosuchia and Neosuchia. Within Thalattosuchia, both Teleosauroidea and Metriorhynchoidea are recovered as monophyletic. *Pelagosaurus typus* is found to be a basal metriorhynchoid, and Metriorhynchidae, Geosaurinae and Geosaurini are all found to be monophyletic (Fig. 11).

Although the three phylogenetic analyses do not recover Thalattosuchia in the same region of the crocodylomorph tree, there are many aspects they do agree upon:

1. The monophyly of Thalattosuchia
2. The separation of Thalattosuchia into two clades: Teleosauroidea and Metriorhynchoidea
3. That *Pelagosaurus typus* is a basal metriorhynchoid
4. The sister group relationship between *P. typus* and *Magyarosuchus fitosi*, which forms the basal-most sub-clade of Metriorhynchoidea
5. The monophyly of Metriorhynchidae

6. The monophyly of Geosaurini

This suggests that the newer, larger, phylogenetic datasets being compiled on thalattosuchian internal relationships are becoming less sensitive to where in Crocodylomorpha Thalattosuchia is recovered. Although all three datasets do have interesting internal differences in the arrangement of Teleosauroidea and the monophyly or not of Metriorhynchinae, there is a growing consensus between them. The recovery of *Steneosaurus gracilirostris* as the basal-most teleosauroid in the H+Y and W matrices (Fig. 10A, 11) is especially interesting, as it polarises laterally oriented orbits as being symplesiomorphic for Thalattosuchia (with the dorsal orientation being a convergence between derived teleosauroids and neosuchians).

Given that, except for *Pelagosaurus typus*, the postcranial anatomy of basal metriorhynchoids is poorly known, we tested whether this species is the sole responsible taxon for pulling the mostly postcranial-based *Magyarosaurus fitosi* among basal metriorhynchoids. The exclusion of *P. typus* from the mA matrix retains *Magyarosaurus fitosi* at the base of Metriorhynchoidea. Excluding *P. typus* from the W and H+Y matrices finds *M. fitosi* close but unresolved relative to other basal metriorhynchoids (in the case of the H+Y matrix only when the highly fragmentary *Peipehsuchus teleorhinus* is removed from the consensus tree) although few of the alternative positions are supported by synapomorphies. The absence of common synapomorphies is due to the lack of *P. typus* and the inclusion of few basal metriorhynchoids in the H+Y/W matrices, all of which lack post-crania and therefore cannot be commonly scored for the post-cranial characters that could unite *M. fitosi* with other metriorhynchoids. The metriorhynchoid affinity of *M. fitosi* is therefore rather reasonable (e.g., presence of enlarged femoral medial tuber; coracoid with convex proximal and distal ends; oval-shaped sacral vertebral centrum) but we cannot exclude that it may be more derived within the group because little is known about character evolution at the base of the clade.

647

648 DISCUSSION

649 **Thalattosuchian marine adaptations**

650 Postcranial elements in basal thalattosuchians (especially in metriorhynchoids Young et al., 2010)
 651 are poorly known, thus the early phases of their adaptation to a fully aquatic lifestyle is still
 652 speculative. Wilberg (2015) listed a number of skeletal adaptations thought to be linked to an
 653 increasingly marine lifestyle in thalattosuchians, such as: 1) the reorientation of the orbit from
 654 dorsal to laterally directed (Hua and Buffrénil, 1996), 2) development of hypertrophied nasal
 655 exocrine glands (Fernández and Gasparini, 2008; ~~Gasparini et al., 2000~~; Gandola et al., 2006), 3)
 656 humerus mediolateral flattening and a reduction in diaphysis length (both in Teleosauroidea and
 657 Metriorhynchoidea), 4) reduction of relative tibia and ulna length, 5) reduction and loss of
 658 osteoderm cover, 6) modification of the pelvis, 7) development of a hypocercal tail with a distinct
 659 regionalisation of the distal caudal vertebrae (Fraas, 1902; Andrews, 1913; Hua and Buffetaut,
 660 1997; Young et al., 2010).

661 *Magyarosuchus* sheds new light on the early evolutionary history of marine adaptations in
 662 Thalattosuchia. Most of the elements in *Magyarosuchus* seem to indicate a body-plan similar to
 663 basal teleosauroids: in having elongated limb bone diaphyses with well-developed proximal and
 664 distal epiphyses, a “primitive” pelvis construction (robust iliac peduncles, retention of iliac
 665 postacetabular process), and the presence of complex and heavy dorsal and ventral osteoderm
 666 cover. The astragalus is very complex with well-developed articulation surfaces for the tibia,
 667 fibula, and metatarsal I, and with the presence of the calcaneal peg it shows the typical
 668 ‘crocodile-normal’ (‘CN’ of Chatterjee, 1978) crurotarsal ankle joint. These features suggest that
 669 adaptation to marine habitats in *Magyarosuchus* could have been similar to that of the Early
 670 Jurassic teleosauroids *Steneosaurus bollensis*, ‘*Steneosaurus*’ *gracilirostris* and *Platysuchus*
 671 *multiscrobiculatus* (Westphal, 1962).

One caudal vertebra (Fig. 5K-P), however, reveals some features still unknown in these teleosauroids or in basal metriorhynchoids. This vertebra is the smallest and distal most element (Fig. 5K-P, 12I) among the preserved caudals. According to the proportion of vertebral centrum height between the dorsal vertebrae and distal caudal vertebrae measured in *Pelagosaurus typus* (MTM M 62 2516), the distal-most preserved caudal of *M. fitosi* represents one of the last 10-15 elements in the caudal series. In *Steneosaurus bollensis* (MTM M 69 242; Westphal, 1962) and *Pelagosaurus typus* (MTM V.52.2516), these caudals have only reduced, anteroposteriorly short, and slightly posteriorly projected neural spines (Fig. 12E-H). The small caudal of *Magyarosuchus*, on the other hand, possesses an anteroposteriorly long and dorsally projecting, elongate neural spine (Fig. 12I). Although the dorsal end of the neural spine and the anterior end of the centrum is missing (Fig. 5N, O), it clearly differs from the distal-most vertebrae of basal teleosauroids or *P. typus*. We suggest that this vertebra represents the bending zone of the distal end of the caudal series to strengthen a still low and primitive tail fin. Tail fins are present e.g. in the metriorhynchids *Metriorhynchus superciliosus* (GPIT RE 9405), ‘*Metriorhynchus*’ *brachyrhynchus* (NHMUK PV R 3804), *Gracilineustes leedsii* (NHMUK PV R 3014), *Rhacheosauus gracilis* (NHMUK PV R 3948) and *Cricosaurus suevicus* (SMNS 9808). An isolated bending zone caudal vertebra is also known for *Torvoneustes carpenteri* (Wilkinson et al., 2008). In these forms three to four vertebrae of the bending zone have at least two to three times longer neural spines than the previous caudals and the centra are slightly bent with shorter ventral margin (Fraas, 1902; Andrews, 1913). The small caudal of *M. fitosi* is missing its anterior part, but, based on the shape of the posterior articulation of the centrum it might have not been as bended as that e.g. in *Metriorhynchus superciliosus*. It seems that in *M. fitosi* the distal tail was still not as ventrally deflected as in metriorhynchids; the neural spines, however, became elongated to stiffen a small, caudal fin. Moreover, these bending zone caudals in metriorhynchids

(and *M. fitosi*) have a centrum that is mediolaterally compressed relative to the pre-bending vertebrae.

This remarkable feature fits well with the mosaic evolution of marine adaptations in thalattosuchians proposed by Wilberg (2015). Since the skull is unknown in *M. fitosi*, no other skeletal modifications refers to a pelagic habit in this form, except for this modified distal caudal. This suggests that a caudal fin supported by a ventrally bended row of distal caudals and a few distal caudals with elongated neural spines should have occurred by the later part of the Early Jurassic, much earlier in thalattosuchian history than the presently available record shows (later part of the Middle Jurassic, Callovian; Young et al., 2010).

Body length

As there is no complete skull, the only metric to establish a body length estimate was femoral length. However, based on teleosauroids, Young et al. (2016) found femoral length to be the more reliable metric for estimating total length of those thalattosuchians. Both femora of *Magyarosuchus fitosi* are broken and partial dissolved. Taking the raw measurements of the femora and using the femoral length vs body length equations of Young et al. (2011, 2016) we get a range of body length values: 4.6–4.8 m. This is based on: 1) difference in size between the left and right femora due to preservation, and 2) the uncertainty of whether to use the metriorhynchid equation from Young et al. (2011) or the two teleosauroids equations of Young et al. (2016). (Note that Young et al. [2016] had two equations: first based on a complete skeleton sample of 12, and a slightly larger sample of 16 with added some less complete skeletons.)

If we assume *M. fitosi* had a scaling ratio similar to teleosauroids, and only use the more complete right femur, this yields a body length estimate of 4.67–4.74 m. However, if *M. fitosi* had a scaling ratio similar to metriorhynchids, and we only use the more complete right femur, this gives a body length estimate of 4.83 m. Interestingly, Young et al. (2016) found using the

metriorhynchid body length equations to more reliably estimate the size of two *Pelagosaurus typus* skeletons. This suggests that basal metriorhynchoids may have had a scaling ratio more similar to metriorhynchids than teleosauroids. However, as the sample was only of two *P. typus* specimens this conclusion remains untested.

Regardless of which equation is correct, a body length of 4.67–4.83 m makes *M. fitosi* the largest known non-metriorhynchid metriorhynchoid. It is substantially larger than the only other Early Jurassic metriorhynchoid *P. typus*, which is typically 2–3 m in length. Furthermore, the fragmentary material of other basal metriorhynchoids all suggest taxa closer in size to *P. typus* than *M. fitosi*, or perhaps reaching 3.5 m (see Eudes-Deslongchamps, 1867–1869; Collot, 1905; Mercier, 1933; Gasparini et al., 2000; Wilberg, 2015; NHMUK PV R 2681, NHMUK PV R 3353). Moreover, these length estimates also mean *M. fitosi* was larger than most metriorhynchid specimens estimated by Young et al. (2011), as few metriorhynchid species exceeded 4.5 m in length, and those that did were the larger-bodied macrophagous taxa.

Compared to known Early Jurassic teleosauroids, *M. fitosi* was within the size range of the larger-bodied species. Few Early Jurassic thalattosuchians are known to exceed 4.5 m, with species such as *Platysuchus multiscrobiculatus* and ‘*Steneosaurus*’ *gracilirostris* typically in the 2–3 m range (see Westphal, 1962; NHMUK PV OR 14792, SMNS 9930). The holotype of ‘*Steneosaurus*’ *brevior* (NHMUK PV OR 14781) is that of a large skull and lower jaw, with an approximate length of 88.3 cm. Using the cranial to body length questions of Young et al. (2016), it has an estimated body length of 4.47–4.58 m. However, there are specimens, which albeit are rare, of *Steneosaurus bollensis* reaching, and even exceeding, 5 m (see Westphal, 1962; Young et al., 2016). Therefore, the largest Early Jurassic thalattosuchians, and crocodylomorphs, were most likely teleosauroids. This trend continues into the Middle Jurassic and on into the Early Cretaceous with teleosauroids reaching greater body lengths than metriorhynchoids (see Young et al., 2016).

746

747 CONCLUSIONS

748 Here, we describe a new crocodylomorph taxon, *Magyarosuchus fitosi* gen. et sp. nov., based on a
 749 new skeleton from the Gerecse mountains of Hungary. Despite being incomplete and lacking the
 750 cranium, we demonstrate that this late Lower Jurassic taxon shows remarkable similarities with
 751 the iconic Lower Jurassic genus *Pelagosaurus*. *Magyarosuchus* and *Pelagosaurus* are found to be
 752 sister taxa in all three phylogenetic analyses undertaken herein, although the two characters
 753 uniting this arrangement are not known from other basal metriorhynchoids (due to poor
 754 preservation of taxa such as *Teleidosaurus*, *Eoneustes* and *Zoneait*). Therefore, we cannot be
 755 certain that the sister relationship between *Magyarosuchus* and *Pelagosaurus* is natural, or due to
 756 incomplete information. Regardless, both are found to be basal metriorhynchoids, near the start
 757 of the radiation that yielded dolphin-like crocodyliforms. Interestingly, *M. fitosi* is the oldest
 758 known thalattosuchian discovered from an "ammonitico rosso" type pelagic deposit (rather than
 759 the usual estuarine, lagoonal or coastal ecosystems Lower Jurassic thalattosuchians are
 760 discovered from). The pelagic depositional environment and neritic associated cephalopod fauna
 761 are both consistent with the inferred open-marine adaptation of *M. fitosi*, namely a mediolaterally
 762 compressed distal caudal vertebra with an usually elongated and dorsally projected neural spine
 763 which suggests the presence of a distal tail structure that could have been a hypocercal fin, or a
 764 precursor to it. The unique combination of retaining heavy dorsal and ventral armor, while having
 765 a slight hypocercal tail, on the other hand, highlights the mosaic manner of marine adaptations in
 766 Metriorhynchoidea. Furthermore, it underscores how little is still known about the timing and
 767 tempo of metriorhynchoid pelagic adaptations and their early radiation.


768

769 Acknowledgements

We thank Attila Fitos, discoverer of the specimen and Z. Sirányi, Z. Szabó and I. Szabó for the excavation and early preparation of the specimen. We are grateful to P. Gulyás, R. Kalmár and M. Szabó (ELTE) for preparation and taking photographs of the specimens, and János Magyar for technical help. We thank L. Kordos (Budapest, Hungary) for his advises given during the project and his comments to an earlier version of the manuscript. MTY would like to thank R. Allain (MNHN), E. Maxwell and R. Schoch (SMNS), D. Schwarz (MfN), D. Vasilyan, I. Werneburg (GPIT) and M. Gasparik and Z. Szentesi (MTM) for collections access during these trips.

REFERENCES

- Adams-Tresman, S. M. 1987. The Callovian (Middle Jurassic) teleosaurid marine crocodiles from central England. *Paleontology* 30(part1):195–206.
- Andrade, M. B., R. Edmonds, M. J. Benton, and R. Schouten. 2011. A new Berriasian species of *Goniopholis* (Mesoeucrocodylia, Neosuchia) from England, and a review of the genus. *Zoological Journal of the Linnean Society* 163:66–108.
- Andrews, C. W. 1913. A Descriptive Catalogue of the Marine Reptiles of the Oxford Clay, Part Two. British Museum (Natural History) Press, London U.K.
- Bernoulli, D., and H. S. Jenkyns. 2009. Ancient oceans and continental margins of the Alpine-Mediterranean Tethys: deciphering clues from Mesozoic pelagic sediments and ophiolites. *Sedimentology* 56:149–190.
- Bronzati, M., F. C. Montefeltro, and M. C. Langer. 2015. Diversification events and the effects of mass extinctions on Crocodyliformes evolutionary history. *Royal Society Open Science* 2:140385. Doi: 10.1098/rsos.140385

- 794 Buffetaut, E. (ed.). 1980. Teleosauridae et Metriorhynchidae: l'évolution de deux familles de
795 Crocodiliens méso-suchiens marins du Mésozoïque. Comptes Rendus du 105e Congrès
796 National des Sociétés Savantes, Caen, France, 12 pp.
- 797 Buffetaut, E. 1982. Radiation évolutive, paléoécologie et biogéographie des crocodiliens
798 méso-suchiens. Mémoires de la Société Géologique de France 142:1–88.
- 799 Buffetaut, E., and R. Ingavat. 1983^a. *Goniopholis phuwiangensis* nov. sp., a new mesosuchian 
800 crocodile from the Mesozoic of northeastern Thailand. Geobios 16(1):79-91.
- 801 Buscalioni, Á. D. 2017. The Gobiosuchidae in the early evolution of Crocodyliformes. Journal of
802 Vertebrate Paleontology 37(3): e1324459. Doi: 10.1080/02724634.2017.1324459
- 803 Chatterjee, S. 1978. A primitive parasuchid (phytosaur) reptile from the Upper Triassic Maleri
804 Formation of India. Paleontology 21(part1):83–127.
- 805 Clark, J. M. 2011. A new shartegosuchid crocodyliform from the Upper Jurassic Morrison
806 Formation of western Colorado. Zoological Journal of the Linnean Society 163:152-172.
- 807 Colbert, E. C., and C. C. Mook. 1951. The ancestral crocodile *Protosuchus*. Bulletin of the
808 American Museum of Natural History 97:143–182.
- 809 Collot, L. 1905. Reptile Jurassique (*Teleidosaurus gaudryi*) trouvé à Saint-Seine-L'Abbaye (Côte-
810 d'or). Mémoires de l'Académie des sciences, arts et belles-lettres Dijon 4(10):41–45.
- 811 Cresta, S., and A. Galácz. 1990. Mediterranean basal Bajocian ammonite faunas. Examples from
812 Hungary and Italy. Memorie Descrittive della Carta Geologica d'Italia 40:165–198.
- 813 Crompton, A. W., and K. K. Smith. 1980. A new genus and species from the Kayenta Formation
814 (Late Triassic?) of Northern Arizona; pp. 193-217 in L. Jacobs (ed.), Aspects of Vertebrate
815 History. Museum of Northern Arizona Press, Flagstaff, Arizona.
- 816 Cruickshank, A. R. I. 1979. The ankle joint in some early archosaurs. South African Journal of
817 Science 75:168–178.

- 818 Császár, G., A. Galácz, and A. Vörös. 1998. Jurassic of the Gerecse Mountains, Hungary: facies
819 and Alpine analogies. *Földtani Közlöny* 128(2-3):397–435.
- 820 Delfino, M., and C. Dal Sasso. 2006. Marine reptiles (Thalattosuchia) from the Early Jurassic of
821 Lombardy (northern Italy). *Geobios* 39:346–354. Doi: 10.1016/j.geobios.2005.01.001
- 822 d’Orbigny, A. 1842–1851. *Paléontologie française, Terrains Jurassique I.: céphalopodes, V.*
823 Masson Press, Paris, France, 642 pp.
- 824 Eudes-Deslongchamps, E. 1867–1869. *Notes Paléontologiques*. Caen and Paris, France, 320–392
825 pp.
- 826 Efimov, M. B. 1975. [Late Cretaceous crocodiles of Soviet Central Asia and Kazakhstan].
827 *Paleontologičeskij žurnal* 9:417–420. [Russian]
- 828 Efimov, M. B. 1988. [On the fossil crocodiles of Mongolia and the Soviet Union]. *Trudy*
829 *Sovmestnaâ Sovetsko-Mongolskaâ Paleontologičeskaâ Ekspediciâ* 34:81–90. [Russian]
- 830 Fernández, M. S., and Z. Gasparini. 2008. Salt glands in the Jurassic metriorhynchid *Geosaurus*:
831 implications for the evolution of osmoregulation in Mesozoic crocodyliforms.
832 *Naturwissenschaften* 95:79–84. Doi: 10.1007/s00114-007-0296-1.
- 833 Fitzinger, L. J. F. J. 1843. *Systema Reptilium*. Vindobonae: Braumüller et Seidel Press, Wien,
834 Austria. ? pp.
- 835 Fodor, L., and I. Főzy. 2013a. Late Middle Jurassic to earliest Cretaceous evolution of basin
836 geometry in the Gerecse Mountains; pp. 117-135 in I. Főzy (ed.), *Late Jurassic – Early*
837 *Cretaceous fauna, biostratigraphy, facies and deformation history of the carbonate formations*
838 *in the Gerecse and Pilis Mountains (Transdanubian Range, Hungary)*. GeoLitera Press,
839 Szeged, Hungary.
- 840 Fodor, L., and I. Főzy. 2013b. The place of the Gerecse Mountains in Alpine-Carpathian
841 framework – A geological setting; pp. 15-20 in I. Főzy (ed.), *Late Jurassic – Early*
842 *Cretaceous fauna, biostratigraphy, facies and deformation history of the carbonate formations*

in the Gerecse and Pilis Mountains (Transdanubian Range, Hungary). GeoLitera Press,
Szeged, Hungary.

Fraas, E. 1901. Die Meerkrokodile (Thalattosuchia n. g.) eine neue Sauriergruppe der
Juraformation. Jahreshefte des Vereins für vaterländische Naturkunde in Württemberg
57:409–418.

Fraas, E. 1902. Die Meer-Krocodilier (Thalattosuchia) des oberen Jura unter specieller
Berücksichtigung von *Dacosaurus* und *Geosaurus*. Palaeontographica 49:1–72.

Galácz, A., G. Császár, B. Géczy, and Z. Kovács. 2010. Ammonite stratigraphy of a Toarcian
(Lower Jurassic) section on Nagy-Pisznice Hill (Gerecse Mts, Hungary). Central European
Geology 53(4):311–342. Doi: 10.1556/CEuGeol.53.2010.4.1

Gandola, R., E. Buffetaut, N. Monaghan, and G. Dyke. 2006. Salt glands in the fossil crocodile
Metriorhynchus. Journal of Vertebrate Paleontology 26:1009–1010. Doi: 10.1671/0272-
4634(2006)26[1009:SGITFC]2.0.CO;2.

Gasparini, Z. B., P. Vignaud, and G. Chong. 2000. The Jurassic Thalattosuchia (Crocodyliformes)
of Chile: a paleobiogeographic approach. Bulletin de la Société Géologique de France
171:657–664.

Goloboff, P., and S. A. Catalano. 2016. TNT version 1.5, including a full implementation of
phylogenetic morphometrics. Cladistics 32:221–238. Doi: 10.1111/cla.12160 32 (3), 221–238

Halliday, T. J., M. B. Andrade, M. J. Benton, and M. B. Efimov. 2013. A re-evaluation of
goniopholidid crocodylomorph material from Central Asia: biogeographic and phylogenetic
implications. Acta Palaeontologica Polonica 60:291–312.

Hay, O. P. 1930. Second bibliography and catalogue of the fossil vertebrata of North America 2.
Carnegie Institute Washington Press, Washington, DC.

- 866 Hua, S. 1999. Le crocodilien *Machimosaurus mosae* (Thalattosuchia, Teleosauridae) du
867 Kimmeridgien du Boulonnais (Pas de Calais, France). *Palaeontographica Abteilung A*
868 252:141–170.
- 869 Hua, S., and E. Buffetaut. 1997. Crocodylia; pp. 357-374 in J. M. Callaway, and E. L. Nicholls
870 (eds.), *Ancient marine reptiles*. Academic Press, San Diego, California.
- 871 Hua, S., and V. Buffrénil. 1996. **Bone histology as a clue in the interpretation of functional**
872 **adaptations in the Thalattosuchia (Reptilia, Crocodylia). *Journal of Vertebrae***
873 ***Paleontology* 16(4):703–717. Doi: 10.1080/02724634.1996.10011359**
- 874 Iordansky, N. N. 1973. The skull of the Crocodilia; pp. 201-262 in C. Gans, and T. S. Parson
875 (eds.), *Biology of the Reptilia, Part 4*. Academia Press, NewYork, New York.
- 876 Johnson, M. M., M. T. Young, L. Steel, D. Foffa, A. S. Smith, S. Hua, P. Havlik, E. A.
877 Howlett, and G. Dyke. 2017. Re-description of ‘*Steneosaurus*’ *obtusidens* Andrews, 1909,
878 an unusual macrophagous teleosaurid crocodylomorph from the Middle Jurassic of
879 England. *Zoological Journal of the Linnean Society* 182(2):385-418.
880 Doi:10.1093/zoolinnea/zlx035
- 881 Kordos, L. 1998. Decouverte d'un crocodile de 180 millions d'années a Gerecse Hongrie.
882 Association Lorraine des Amis des Sciences de la Terre 100:35-38.
- 883 Leardi, J. M., D. Pol, and J. M. Clark. 2017. Detailed anatomy of the braincase of *Macelognathus*
884 *vagans* Marsh, 1884 (Archosauria, Crocodylomorpha) using high resolution tomography and
885 new insights on basal crocodylomorph phylogeny. *PeerJ* 5:e2801. Doi: 10.7717/peerj.2801
- 886 Lucas, S. G., and R. M. Sullivan. 2003. A new crocodilian from the Upper Cretaceous of the San
887 Juan Basin, New Mexico. *Neues Jahrbuch fur Geologie und Palaontologie, Monatshefte*
888 2:109–119.

- 889 Lukeneder, A. 2015. Ammonoid habitats and life history; pp. 689-792 in C. Klug, D. Korn, K.
890 De Baets, I. Kruta, and R. H. Mapes (eds.), Ammonoid Paleobiology. From Anatomy to
891 Ecology. Topics in Geobiology 43. Springer Press, Berlin, Germany.
- 892 Massare, J. A. 1988. Swimming Capabilities of Mesozoic Marine Reptiles: implications for
893 Method of Predation. Paleobiology 14(2):187–205. Doi: 10.1017/S009483730001191X
- 894 Mercier, J. 1933. Contribution à l'étude des Métriorhynchidés (crocodiliens). Annales de
895 Paléontologie 22:99–119.
- 896 Mueller-Töwe, I. J. 2006. Anatomy, phylogeny, and palaeoecology of the basal thalattosuchians
897 (Mesoeucrocodylia) from the Liassic of Central Europe. Unpublished PhD dissertation, 422
898 pp.
- 899 Nash, D. 1968. A crocodile from the Upper Triassic of Lesotho. Journal of Zoology 156(2):163–
900 179. **Doi: 10.1111/j.1469-7998.1968.tb05927.x**
- 901 Narváez, I., C. A. Brochu, F. Escaso, A. Pérez-García, and F. Ortega. 2015. New crocodyliforms
902 from Southwestern Europe and definition of a diverse clade of European Late Cretaceous
903 basal eusuchians. PLoS ONE 10(11):e0140679. Doi: 10.1371/journal.pone.0140679
- 904 Nesbitt, N. J. 2011. The early evolution of archosaurs: relationships and the origin of major
905 clades. Bulletin of the American Museum of Natural History 352:1–292.
- 906 Nesbitt, N. J., and J. B. Desojo. 2017. The osteology and phylogenetic position of *Luperosuchus*
907 *fractus* (Archosauria: Loricata) from the latest Middle Triassic or earliest Late Triassic of
908 Argentina. Ameghiniana 54(3):261–282.
- 909 Ősi, A., M. Rabi, L. Kordos, and A. Fitos. 2010. The crocodyliform from the Gerecse Mountains:
910 the most complete *Steneosaurus* (Thalattosuchia: Teleosauridae) skeleton from the Alp
911 Liassic. 13. Annual Meetings of Hungarian Paleontologists, Csákvár, p. 20-21.

- 912 Parrish, J. M. 1987. The origin of crocodilian locomotion. *Paleobiology* 13(4):369–414. Doi:
913 10.1017/S0094837300009003
- 914 Pierce, S. E., and M. J. Benton. 2006. *Pelagosaurus typus* Bronn, 1841 (Mesoeucrocodylia:
915 Thalattosuchia) from the Upper Lias (Toarcian, ower Jurassic) of Somerset, England. *Journal*
916 *of Vertebrate Paleontology* 26:621–635. Doi: 10.1671/0272-
917 4634(2006)26[621:PTBMTF]2.0.CO;2
- 918 Puértolas-Pascual, E., J. I. Canudo, and L. M. Sender. 2015. New material from a huge specimen
919 of *Anteophthalmosuchus* cf. *escuchae* (Goniopholididae) from the Albian of Andorra (Teruel,
920 Spain): phylogenetic implications. *Journal of Iberian Geology* 41:41–56.
- 921 Ristevski, J., M. T. Young, M. B. Andrade, and A. K. Hastings. 2018. A new species of
922 *Anteophthalmosuchus* (Crocodylomorpha, Goniopholididae) from the Lower Cretaceous of
923 the Isle of Wight, United Kingdom, and a review of the genus. *Cretaceous Research* 84:340–
924 383.
- 925 Romer, A.S. 1972. The Chañares (Argentina) Triassic reptile fauna. An early ornithosuchid
926 pseudosuchian, *Gracilisuchus stipanicorum*, gen. et sp. nov. *Breviora* 389:1–24.
- 927 Schaeffer, B. 1941. The morphological and functional evolution of the tarsus in amphibians and
928 reptiles. *Bulletin of the American Museum of Natural History* 78:395–472.
- 929 Sereno, P. C., and A. B. Arucci. 1990. The monophyly of crurotarsal archosaurs and the origin of
930 bird and crocodile ankle joints. *Neues Jahrbuch für Geologie und Paläontologie*,
931 *Abhandlungen* 180(1):21–52.
- 932 Sertich, J. J. W., and J. R. Groenke. 2010. Appendicular skeleton of *Simosuchus clarki*
933 (Crocodyliformes: Notosuchia) from the Late Cretaceous of Madagascar. *Journal of*
934 *Vertebrate Paleontology* 30(sp1):122–153. Doi: 10.1080/02724634.2010.516902
- 935 Tykoski, R. S., T. B. Rowe, R. A. Ketcham, and M. W. Colbert. 2002. *Calsoyasuchus valliceps*, a
936 new crocodyliform from the Early Jurassic Kayenta Formation of Arizona. *Journal of*

Vertebrate Paleontology 22:593–611. Doi: 10.1671/0272-

4634(2002)022[0593:CVANCF]2.0.CO;2

Vörös, A., and A. Galácz. 1998. Jurassic paleogeography of the Transdanubian Central Range (Hungary). *Rivista Italiana di Paleontologia e Stratigrafia* 104(1):69–84.

Westermann, G. E. G. 1990. New developments in ecology of Jurassic-Cretaceous ammonites; pp. 459–478 in G. Pallini, F. Cecca, S. Cresta, and M. Santantonio (eds.), *Atti del secondo convegno internazionale Fossili, Evoluzione, Ambiente, Pergola*, 25–30 October 1987.

Westphal, F. 1962. Die krokodilier des Deutschen und Englischen oberen Lias. *Palaeontographica* A 116:23–118.

Wilberg, E. W. 2015. A new metriorhynchoid (Crocodylomorpha, Thalattosuchia) from the Middle Jurassic of Oregon and the evolutionary timing of marine adaptations in thalattosuchian crocodylomorphs. *Journal of Vertebrate Paleontology* 35(2):e902846. Doi: 10.1080/02724634.2014.902846.

Wilberg, E.W. 2017. Investigating patterns of crocodyliform cranial disparity through the Mesozoic and Cenozoic. *Zoological Journal of the Linnean Society* 181:189–208.

Wilkinson, L. E., M. T. Young, and M. J. Benton. 2008. A new metriorhynchid crocodile (Mesoeucrocodylia: Thalattosuchia) from the Kimmeridgian (Upper Jurassic) of Wiltshire, U.K. *Palaeontology* 51:1307–1333.

Young, M. T., and M. B. Andrade. 2009. What is *Geosaurus*? Redescription of *Geosaurus giganteus* (Thalattosuchia: Metriorhynchidae) from the Upper Jurassic of Bayern, Germany. *Zoological Journal of the Linnean Society* 157(3):551–585. Doi: 10.1111/j.1096-3642.2009.00536.x

Young, M. T., M. A. Bell, M. B. Andrade, and S. L. Brusatte. 2011. Body size estimation and evolution in metriorhynchid crocodylomorphs: implications for species diversification and niche partitioning. *Zoological Journal of the Linnean Society* 163:1199–1216.

Young, M. T., S. L. Brusatte, M. Ruta, and M. B. Andrade. 2010. The evolution of Metriorhynchoidea (Mesoeucrocodylia, Thalattosuchia): an integrated approach using geometrics morphometrics, analysis of disparity and biomechanics. *Zoological Journal of the Linnean Society* 158:801–859. Doi: 10.1111/j.1096-3642.2009.00571.x

Young, M. T., S. Hua, L. Steel, D. Foffa, S. L. Brusatte, S. Thüring, O. Mateus, J. I. Ruiz-Omeñaca, P. Havlik, Y. Lepage, and M. B. Andrade. 2014. Revision of the Late Jurassic teleosaurid genus *Machimosaurus* (Crocodylomorpha, Thalattosuchia). *Royal Society Open Science* 1:140222.

Young, M. T., M. Rabi, M. A. Bell, L. Steel, D. Foffa, S. Sachs, and K. Peyer. 2016. Big-headed marine crocodyliforms, and why we must be cautious when using extant species as body length proxies for long extinct relatives. *Palaeontologia Electronica* 19.3.30A:1–14.

Figure and table captions:

Figure 1. Locality map of the new thalattosuchian crocodyliform, *Magyarosuchus fitosi* gen. et sp. nov. from the Toarcian of the Gerecse Mountains, Hungary. Red point marks the fossil site.

Figure 2. Schematic geological section of the locality at the Nagy-Pisznice Hill, close to Békás-Canyon (GPS coordinates: 47°42'09.4"N, 18°29'40.0"E), eastern Gerecse Mountains, northwestern Hungary. The Upper Toarcian fossiliferous bed (Bed 13) produced the remains of the new thalattosuchian *Magyarosuchus fitosi* gen. et sp. nov.

Figure 3. Mandibular elements of *Magyarosuchus fitosi* gen. et sp. nov. from the Toarcian of the Gerecse Mountains, Hungary. A, left dentale fragment (MTM V.97.2.A), middle portion in

lateral; B, dorsal views. C, left dentale fragment (MTM V.97.2.B), posterior portion in lateral; D, dorsal; E, medial views. F, dorsal (dentale+surangular) and ventral (angular) margins of the mandibular fenestra of the left mandible (MTM V.97.40) in dorsal; G, medial; H, lateral; I, ventral views. Note that the upper and lower margins were compressed to each other preventing to outline the external mandibular fenestra. J, Right? mandible fragment (MTM V.97.2.C) in dorsal; K, ventral; L, lateral views. Abbreviations: al, alveolus; an, angular; emf, external mandibular fenestra. gr, groove; maf, mandibular adductor fossa; sa, surangular; sh, shelf.

Figure 4. Teeth of *Magyarosuchus fitosi* gen. et sp. nov. from the Toarcian of the Gerecse Mountains, Hungary. A, anterior tooth with root fragment in labial view. B, anterior or middle tooth with root in mesial/distal view. C, posterior tooth (MTM V.97.1) with root in labial; D, lingual; E, ?mesial; F, distal views. G, Middle or posterior tooth in mesial/distal views. H-I, details of the ornamentation and the unserrated carina. Abbreviations: c, carina; ec, end of the carina; wr, wrinkle.

Figure 5. Axial elements of *Magyarosuchus fitosi* gen. et sp. nov. from the Toarcian of the Gerecse Mountains, Hungary. A, dorsal vertebra (MTM V.97.26) in right lateral; B, ventral; C, anterior views. D, sacrum with the last dorsal (lumbar) and the first caudal vertebra (MTM V.97.30) in right lateral; E, ventral views. F, middle caudal vertebra (MTM V.97.28) in right lateral; G, anterior; H, ventral views. I, distal caudal vertebra (MTM V.97.31) in anterior, J, right lateral views. K, distal caudal vertebra (MTM V.97.19.) with massive neural spine in right lateral; L, left lateral; M, posterior; N, anterior; O, dorsal; P, ventral views. Abbreviations: ansp, anterior process of the neural spine; ca1, first caudal vertebra; ld, last dorsal vertebra; nc, neural canal; nsp, neural spine; pns, posterior process of neural spine; prz, prezygapophysis; sa1-2, sacral vertebrae 1-2; sra1-2, articulation for sacral ribs 1-2; trp, transverse process.

1012

1013 **Figure 6.** Appendicular elements of *Magyarosuchus fitosi* gen. et sp. nov. from the Toarcian of
1014 the Gerecse Mountains, Hungary. A, fragmentary dorsal rib (MTM V.97.8) in anterior; B,
1015 posterior views. C, sacral rib (MTM V.97.37) in anterior/posterior; D, medial views. , E, sacral
1016 rib (MTM V.97.39) in anterior/posterior; F, medial views. G, coracoid (MTM V.97.7) in ventral
1017 view. H, glenoid of the coracoid (MTM V.97.7). I, left ilium (MTM V.97.34) in anterior; J,
1018 laterodorsal; K, posterior; L, lateral views. M, right ilium (MTM V.97.44) in medial view. N, left
1019 pubis (MTM V.97.35) in anterodorsal; O, lateral views. P, distal half of the left ischium (MTM
1020 V.97.36) in lateral view. Abbreviations: ac, acetabulum; as, articulation surface; ca, capitulum; cf,
1021 coracoid foramen; gl, glenoid; ic, iliac crest; isa, articulation surface for ischium; prp,
1022 preacetabular process; pop, postacetabular process; sra, articulation surface for sacral rib; t,
1023 tuberculum.

1024

1025 **Figure 7.** Limb elements of *Magyarosuchus fitosi* gen. et sp. nov. from the Toarcian of the
1026 Gerecse Mountains, Hungary. A, proximal end of radius (MTM V.97.42) in ?lateral; B, ?medial
1027 views. C, a short limb bone (?metacarpal or ?ulnare) with distal articular surface (left) associated
1028 with a dorsal rib (central) and a third bone fragment (right) (MTM V.97.38). D, left femur (MTM
1029 V.97.13) in lateral; E, medial; F, posterior; G, anterior; H, proximal; I, distal views. J, left tibia
1030 (MTM V.97.9.) in posterior; K, medial; L, lateral; M, anterior; N, proximal; O, distal views. P,
1031 proximal end of fibula (MTM V.97.15) in medial; Q, lateral; R, proximal views. S, distal end of
1032 fibula (MTM V.97.43) in lateral; T, medial views. Abbreviations: as, articular surface; cnc,
1033 cnemial crest; dr, dorsal rib fragment; fh, femoral head; mco, medial condyle; lco, lateral
1034 condyle; mx, matrix; pra, proximal articulation surface.

1035

Figure 8. Limb elements of *Magyarosuchus fitosi* gen. et sp. nov. from the Toarcian of the Gerecse Mountains, Hungary. A, left astragalus (MTM V.97.12) in posterior; B, anterior; C, dorsal; D, ventral; E, lateral; F, medial views. G, metatarsal III (MTM V.97.10) in proximal; H, distal; I, posterior; J, lateral/medial views. K, phalanges (MTM V.97.61) in dorsal; K, ventral views. M, unidentified limb bone element (?distal end of fibula?). Abbreviations: amt1, articulation surface for metatarsal I; cap, calcaneal peg; fia, fibular articulation surface; fo, foramen; tia, tibial articulation surface.

Figure 9. Osteoderms of *Magyarosuchus fitosi* gen. et sp. nov. from the Toarcian of the Gerecse Mountains, Hungary. A, dorsal osteoderm (MTM V.97.59) in dorsal; B, posterior; C, posteromediodorsal views. D, dorsal osteoderm (MTM V.97.60) in dorsal view. E, dorsal osteoderm (MTM V.97.60) in dorsal; F, posterior views. G, block of six ventral osteoderms (MTM V.97.38) in ventral; H, anteroventral views. I, block of two ventral osteoderms (MTM V.97.38) in ventral view. Abbreviations: aar, anterior articulation surface; alp, anterolateral process; lcr, lateral crest; su, suture.

Figure 10. Results of the phylogenetic analyses. A, Strict consensus of 84 most parsimonious cladograms based on the Hastings + Young matrix (Young et al., 2016), showing the phylogenetic relationships of *Magyarosuchus fitosi* gen. et sp. nov. within Metriorhynchoidea. B, Strict consensus of 16 most parsimonious cladograms based on the modified Andrade matrix (Andrade et al., 2011), showing the phylogenetic relationships of *Magyarosuchus fitosi* gen. et sp. nov. within Metriorhynchoidea.

Figure 11. Strict consensus of six most parsimonious cladograms based on the Wilberg matrix (Wilberg, 2017), showing the phylogenetic relationships of *Magyarosuchus fitosi* gen. et sp. nov. within Metriorhynchoidea.

Figure 12. Comparison of thalattosuchian bony tails and the distal caudal vertebrae within the bending zone. A-B, *Cricosaurus suevicus* from Nusplingen (GPIT RE 7322); C-D, *Metriorhynchus superciliosus* (GPIT RE 9405); E-F, *Steneosaurus bollensis* (MTM M 69 242) ; G-H, *Pelagosaurus typus* (MTM M 62 2516); I, *Magyarosaurus fitosi* gen. et sp. nov. distal caudal (MTM V.97.19.) with the interpreted original outline of the vertebra.

Table 1. Measurements of the bones of *Magyarosuchus fitosi* gen. et sp. nov. from the Toarcian of the Gerecse Mountains, Hungary.

Figure 1(on next page)

Locality map of the new thalattosuchian crocodyliform, *Magyarosuchus fitosi* gen. et sp. nov. from the Toarcian of the Gerecse Mountains, Hungary.

Red point marks the fossil site.

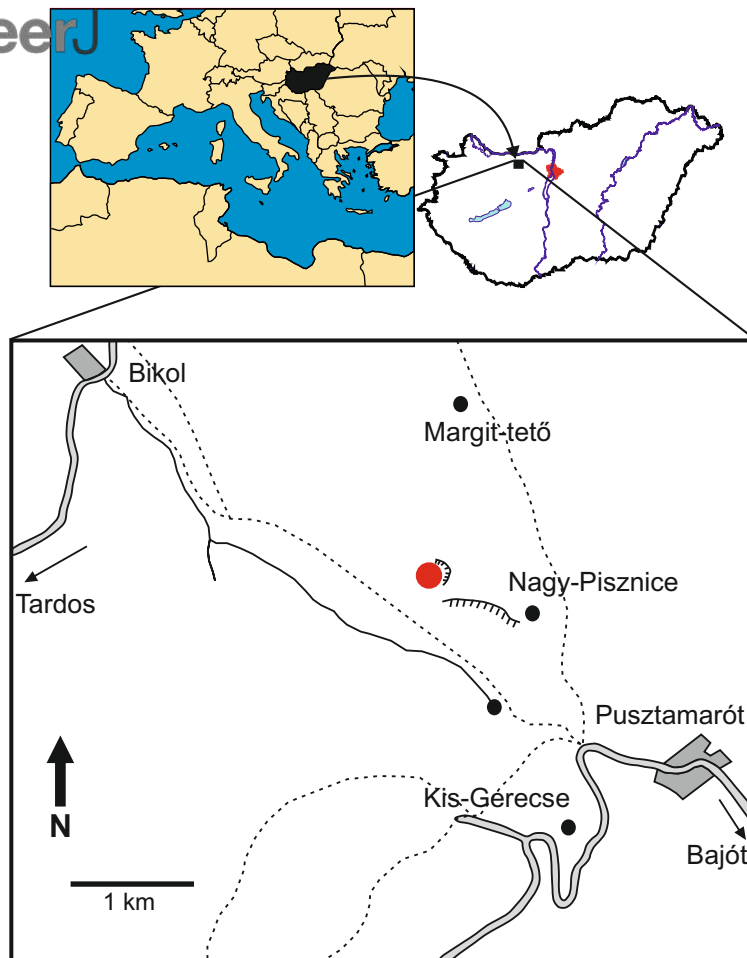


Figure 2 (on next page)

Schematic geological section of the locality at the Nagy-Pisznice Hill, close to Békás-Canyon (GPS coordinates: 47°42'09.4"N, 18°29'40.0"E), eastern Gerecse Mountains, northwestern Hungary.

The Upper Toarcian fossiliferous bed (Bed 13) produced the remains of the new thalattosuchian *Magyarosuchus fitosi* gen. et sp. nov.

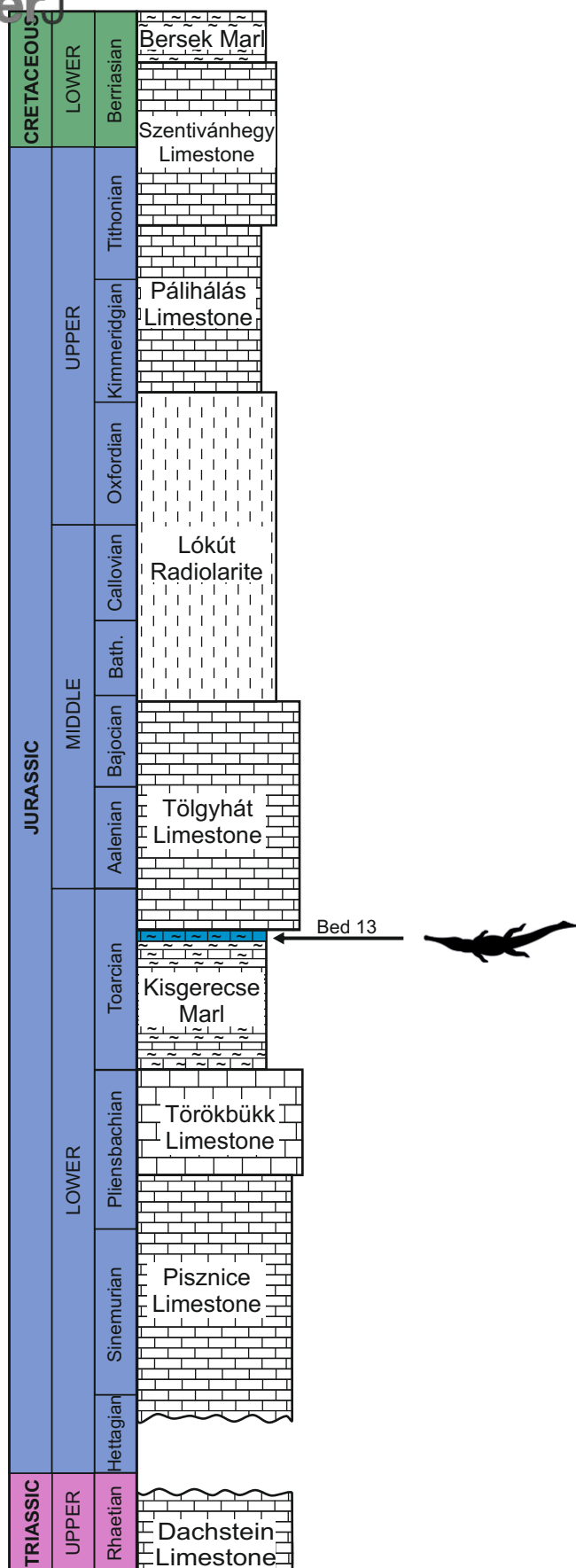


Figure 3

Mandibular elements of *Magyarosuchus fitosi* gen. et sp. nov. from the Toarcian of the Gerecse Mountains, Hungary.

A, left **dentale** fragment (MTM V.97.2.A), middle portion in lateral; B, dorsal views. C, left dentale fragment (MTM V.97.2.B), posterior portion in lateral; D, dorsal; E, medial views. F, dorsal **(dentale+surangular) and ventral (angular)** margins of the mandibular fenestra of the left mandible (MTM V.97.40) in dorsal; G, medial; H, lateral; I, ventral views. Note that the upper and lower margins were compressed to each other preventing to outline the external mandibular fenestra. J, Right? mandible fragment (MTM V.97.2.C) in dorsal; K, ventral; L, lateral views. Abbreviations: al, alveolus; an, angular; emf, external mandibular fenestra, gr, ~~X~~ groove; maf, mandibular adductor fossa; sa, surangular; sh, shelf.

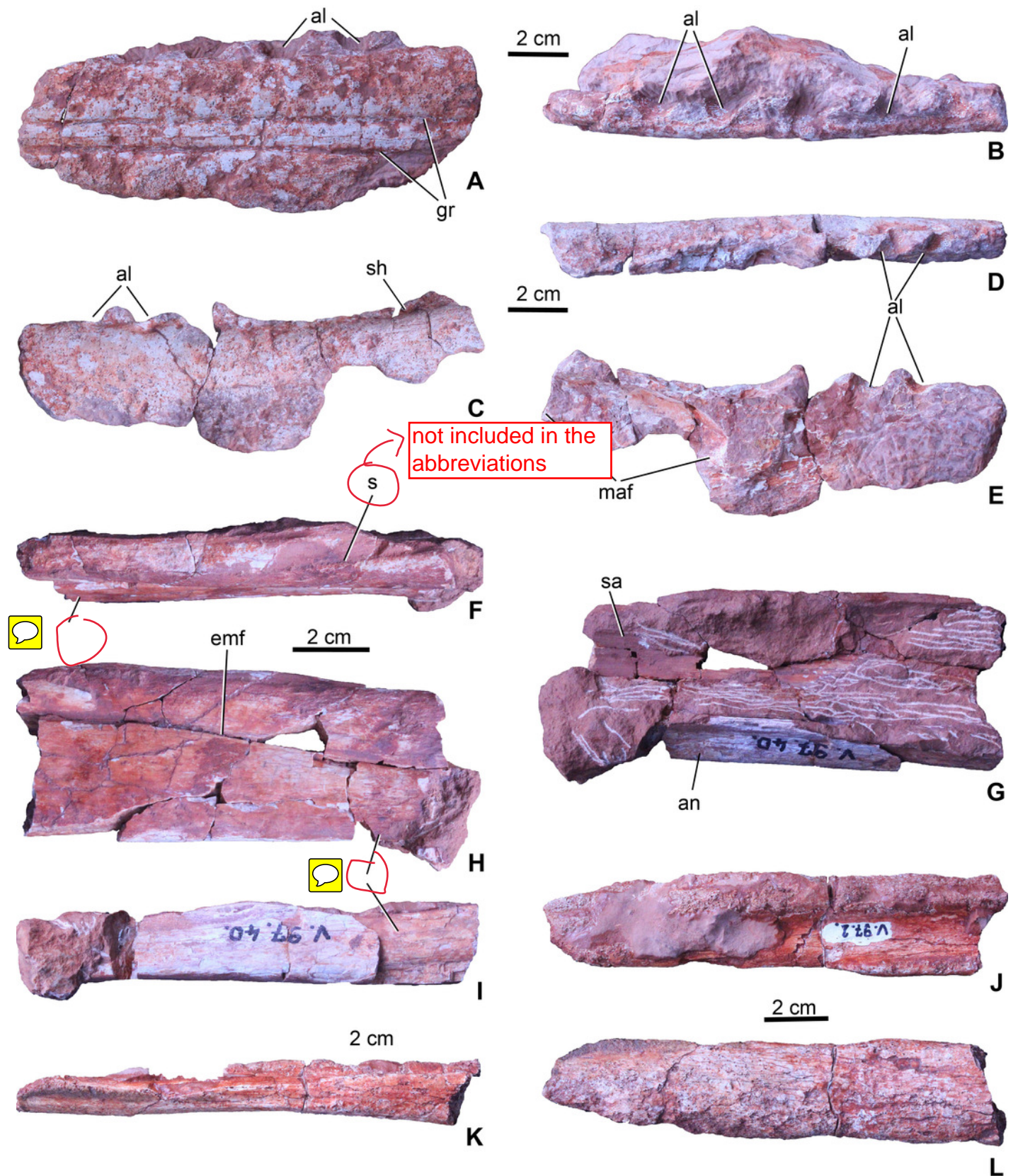


Figure 4

Teeth of *Magyarosuchus fitosi* gen. et sp. nov. from the Toarcian of the Gerecse Mountains, Hungary.

A, anterior tooth with root fragment in labial view. B, anterior or middle tooth with root in mesial/distal view. C, posterior tooth (MTM V.97.1) with root in labial; D, lingual; E, ?mesial; F, distal views. G, Middle or posterior tooth in mesial/distal views. H-I, details of the ornamentation and the unserrated carina. Abbreviations: c, carina; ec, end of the carina; wr, wrinkle.

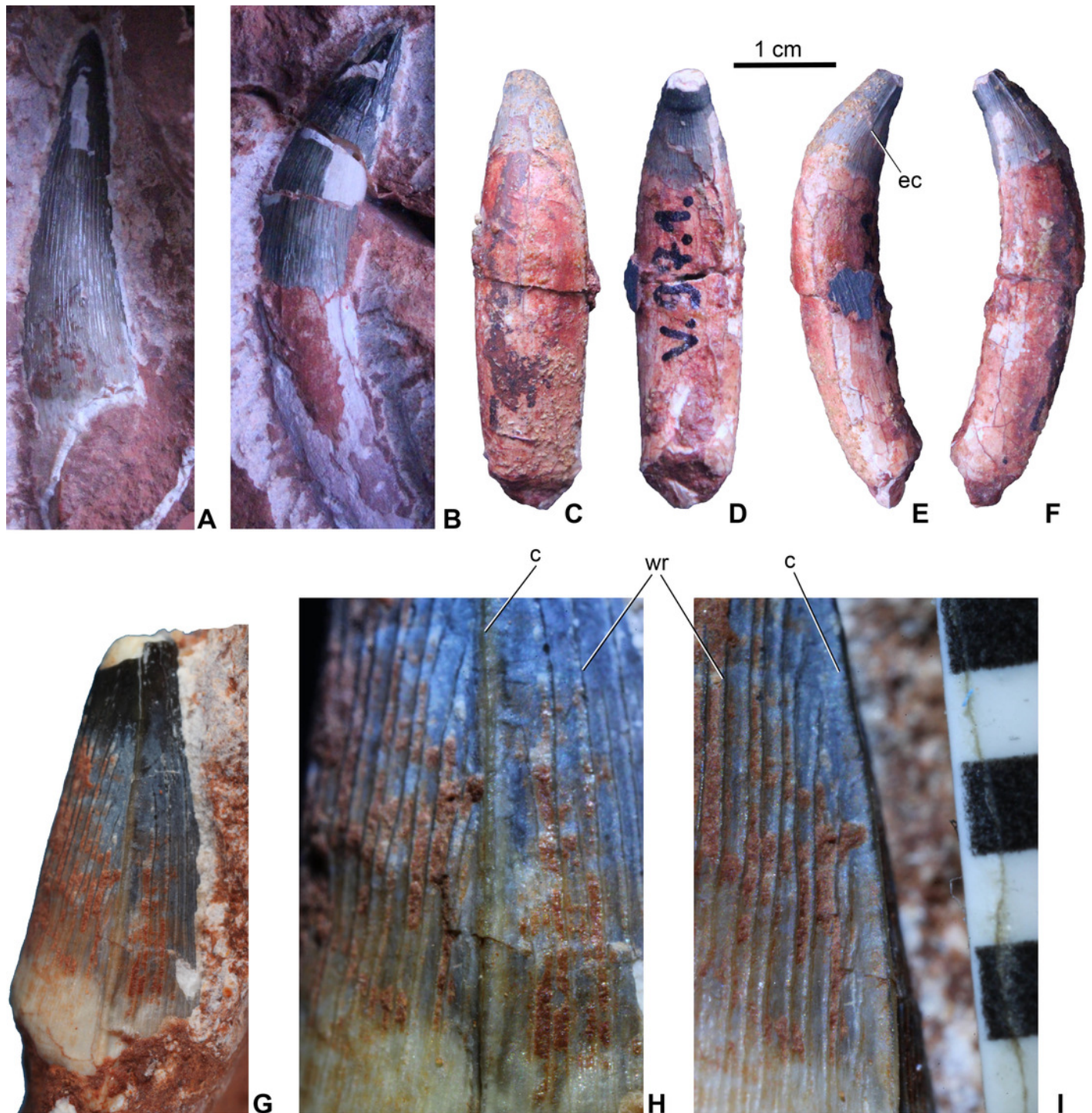


Figure 5

Axial elements of *Magyarosuchus fitosi* gen. et sp. nov. from the Toarcian of the Gerecse Mountains, Hungary.

A, dorsal vertebra (MTM V.97.26) in right lateral; B, ventral; C, anterior views. D, sacrum with the last dorsal (lumbar) and the first caudal vertebra (MTM V.97.30) in right lateral; E, ventral views. F, middle caudal vertebra (MTM V.97.28) in right lateral; G, anterior; H, ventral views. I, distal caudal vertebra (MTM V.97.31) in anterior, J, right lateral views. K, distal caudal vertebra (MTM V.97.19.) with massive neural spine in right lateral; L, left lateral; M, posterior; N, anterior; O, dorsal; P, ventral views. Abbreviations: ansp, anterior process of the neural spine; ca1, first caudal vertebra; ld, last dorsal vertebra; nc, neural canal; nsp, neural spine; pnsp, posterior process of neural spine; prz, prezygapophysis; sa1-2, sacral vertebrae 1-2; sra1-2, articulation for sacral ribs 1-2; trp, transverse process.

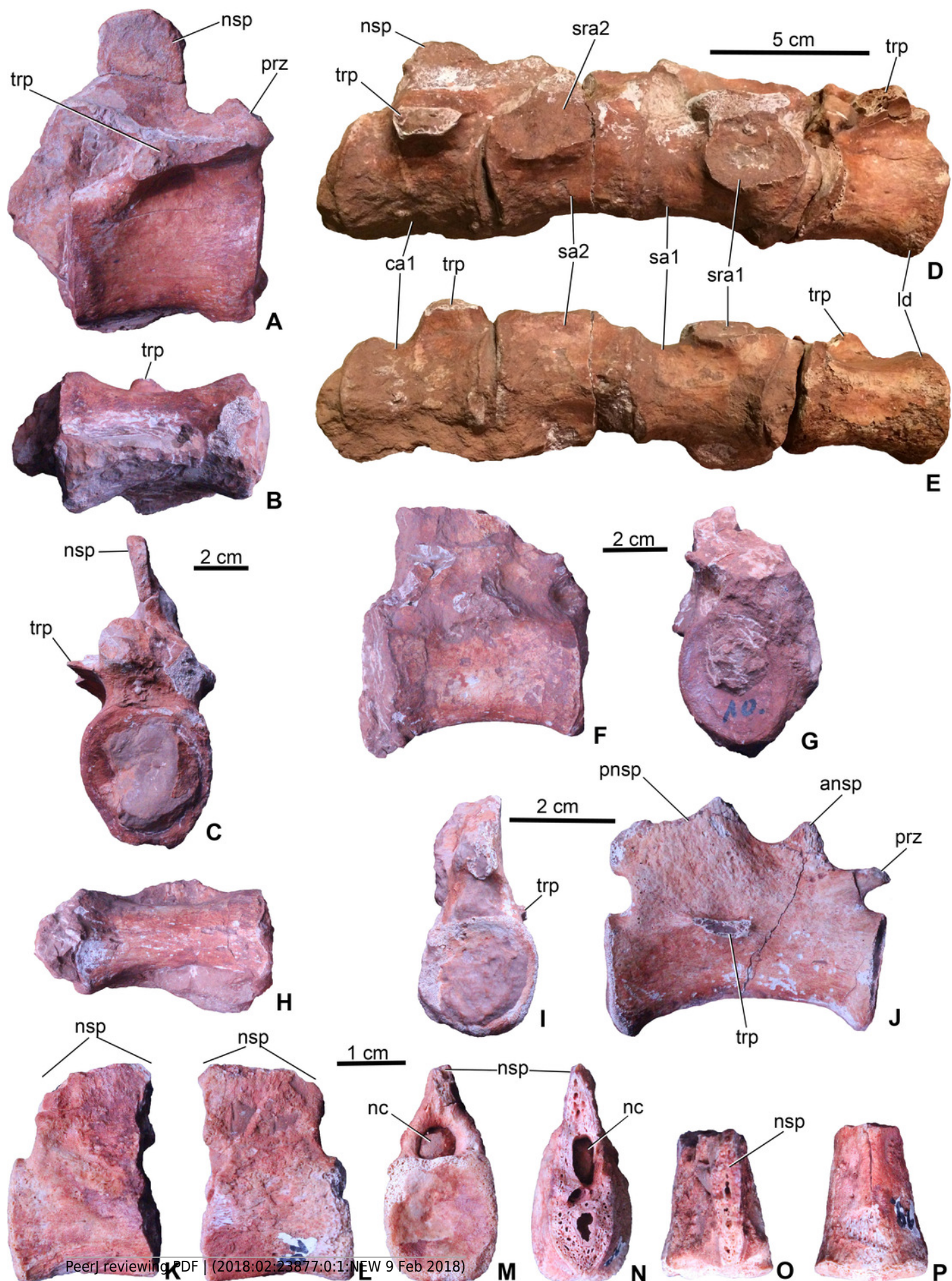


Figure 6

Appendicular elements of *Magyarosuchus fitosi* gen. et sp. nov. from the Toarcian of the Gerecse Mountains, Hungary.

A, fragmentary dorsal rib (MTM V.97.8) in anterior; B, posterior views. C, sacral rib (MTM V.97.37) in anterior/posterior; D, medial views. E, sacral rib (MTM V.97.39) in anterior/posterior; F, medial views. G, coracoid (MTM V.97.7) in ventral view. H, glenoid of the coracoid (MTM V.97.7). I, left ilium (MTM V.97.34) in anterior; J, laterodorsal; K, posterior; L, lateral views. M, right ilium (MTM V.97.44) in medial view. N, left pubis (MTM V.97.35) in anterodorsal; O, lateral views. P, distal half of the left ischium (MTM V.97.36) in lateral view. Abbreviations: ac, acetabulum; as, articulation surface; ca, capitulum; cf, coracoid foramen; gl, glenoid; ic, iliac crest; isa, articulation surface for ischium; prp, preacetabular process; pop, postacetabular process; sra, articulation surface for sacral rib; t, tuberculum.

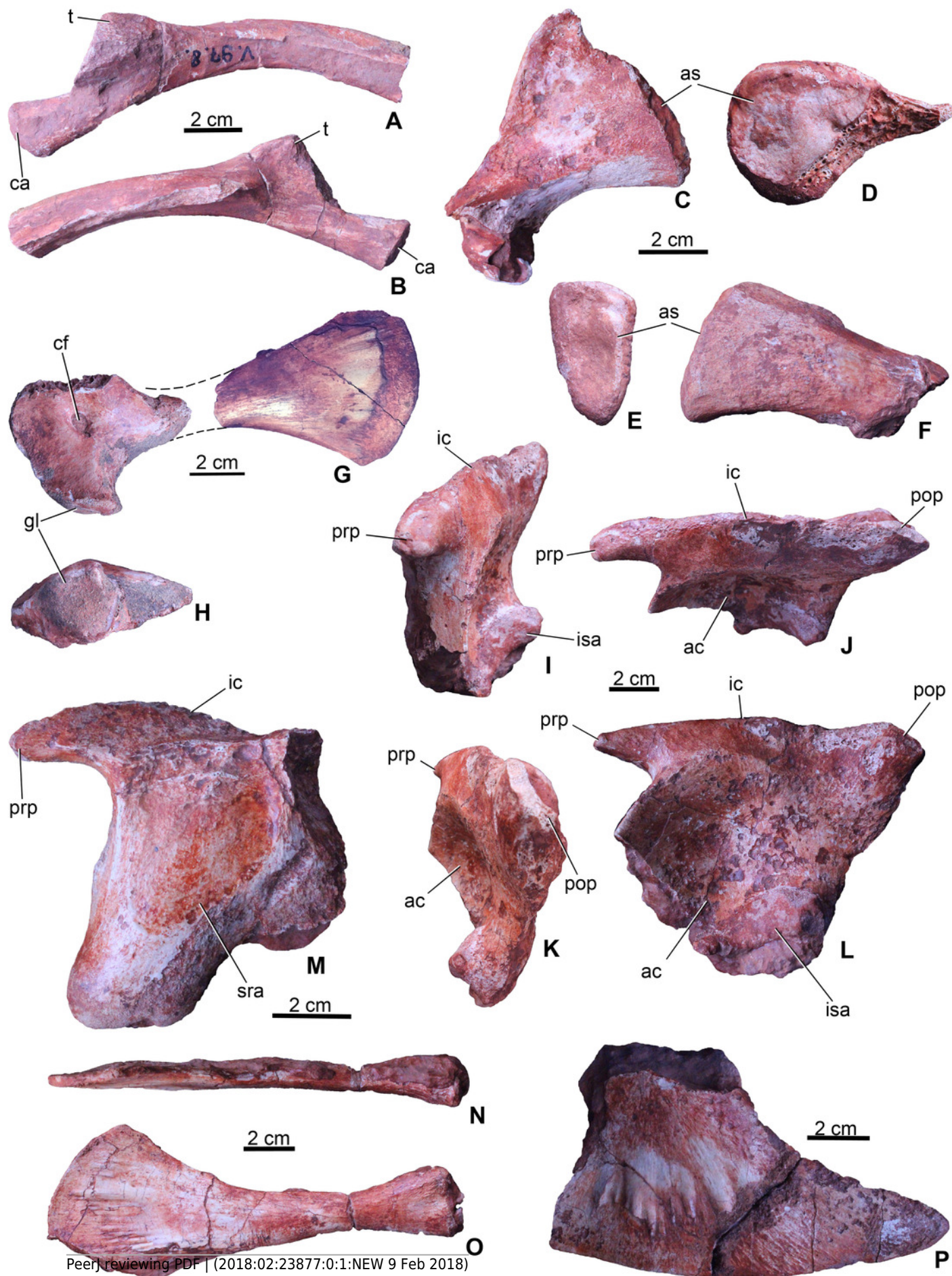


Figure 7

Limb elements of *Magyarosuchus fitosi* gen. et sp. nov. from the Toarcian of the Gerecse Mountains, Hungary.

A, proximal end of radius (MTM V.97.42) in ?lateral; B, ?medial views. C, a short limb bone (?metacarpal or ?ulnare) with distal articular surface (left) associated with a dorsal rib (central) and a third bone fragment (right) (MTM V.97.38). D, left femur (MTM V.97.13) in lateral; E, medial; F, posterior; G, anterior; H, proximal; I, distal views. J, left tibia (MTM V.97.9.) in posterior; K, medial; L, lateral; M, anterior; N, proximal; O, distal views. P, proximal end of fibula (MTM V.97.15) in medial; Q, lateral; R, proximal views. S, distal end of fibula (MTM V.97.43) in lateral; T, medial views. Abbreviations: as, articular surface; cnc, cnemial crest; dr, dorsal rib fragment; fh, femoral head; mco, medial condyle; lco, lateral condyle; mx, matrix; pra, proximal articulation surface.

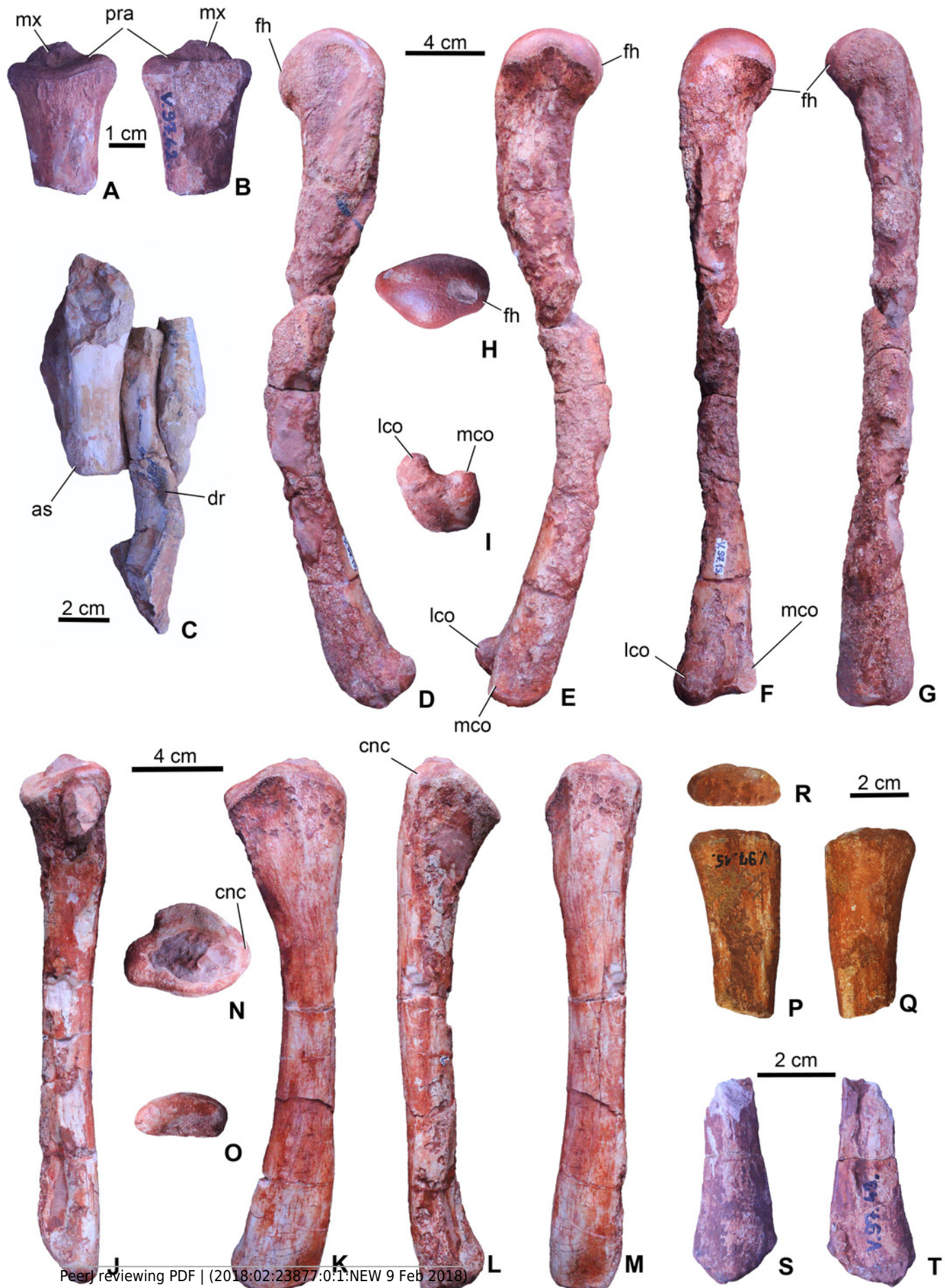


Figure 8

Limb elements of *Magyarosuchus fitosi* gen. et sp. nov. from the Toarcian of the Gerecse Mountains, Hungary.

A, left astragalus (MTM V.97.12) in posterior; B, anterior; C, dorsal; D, ventral; E, lateral; F, medial views. G, metatarsal III (MTM V.97.10) in proximal; H, distal; I, posterior; J, lateral/medial views. K, phalanges (MTM V.97.61) in dorsal; K, ventral views. M, unidentified limb bone element (?distal end of fibula?). Abbreviations: amt1, articulation surface for metatarsal I; cap, calcaneal peg; fia, fibular articulation surface; fo, foramen; tia, tibial articulation surface.

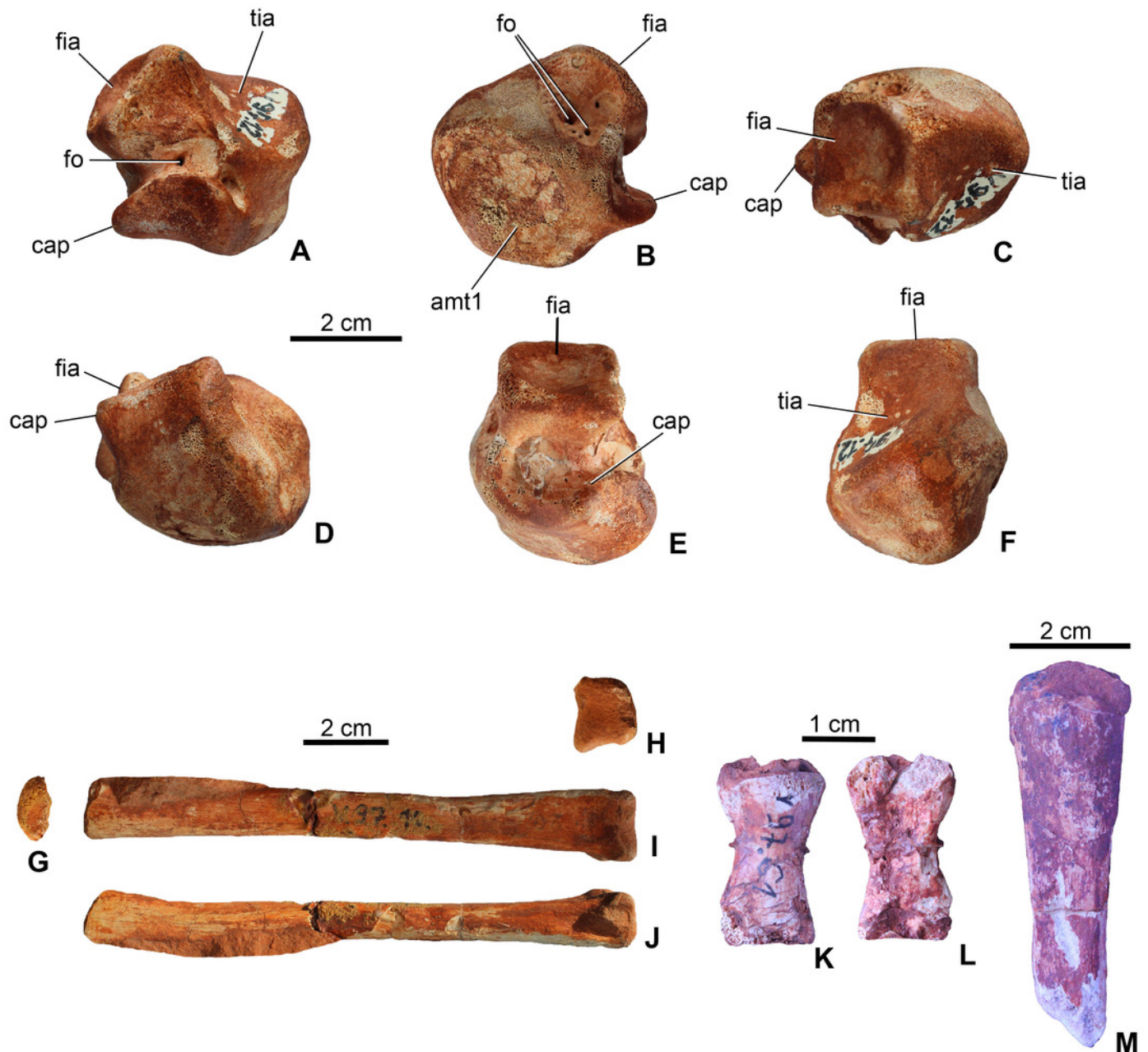


Figure 9

Osteoderms of *Magyarosuchus fitosi* gen. et sp. nov. from the Toarcian of the Gerecse Mountains, Hungary.

A, dorsal osteoderm (MTM V.97.59) in dorsal; B, posterior; C, posteromediodorsal views. D, dorsal osteoderm (MTM V.97.60) in dorsal view. E, dorsal osteoderm (MTM V.97.60) in dorsal; F, posterior views. G, block of six ventral osteoderms (MTM V.97.38) in ventral; H, anteroventral views. I, block of two ventral osteoderms (MTM V.97.38) in ventral view.

Abbreviations: aar, anterior articulation surface; alp, anterolateral process; lcr, lateral crest; su, suture.

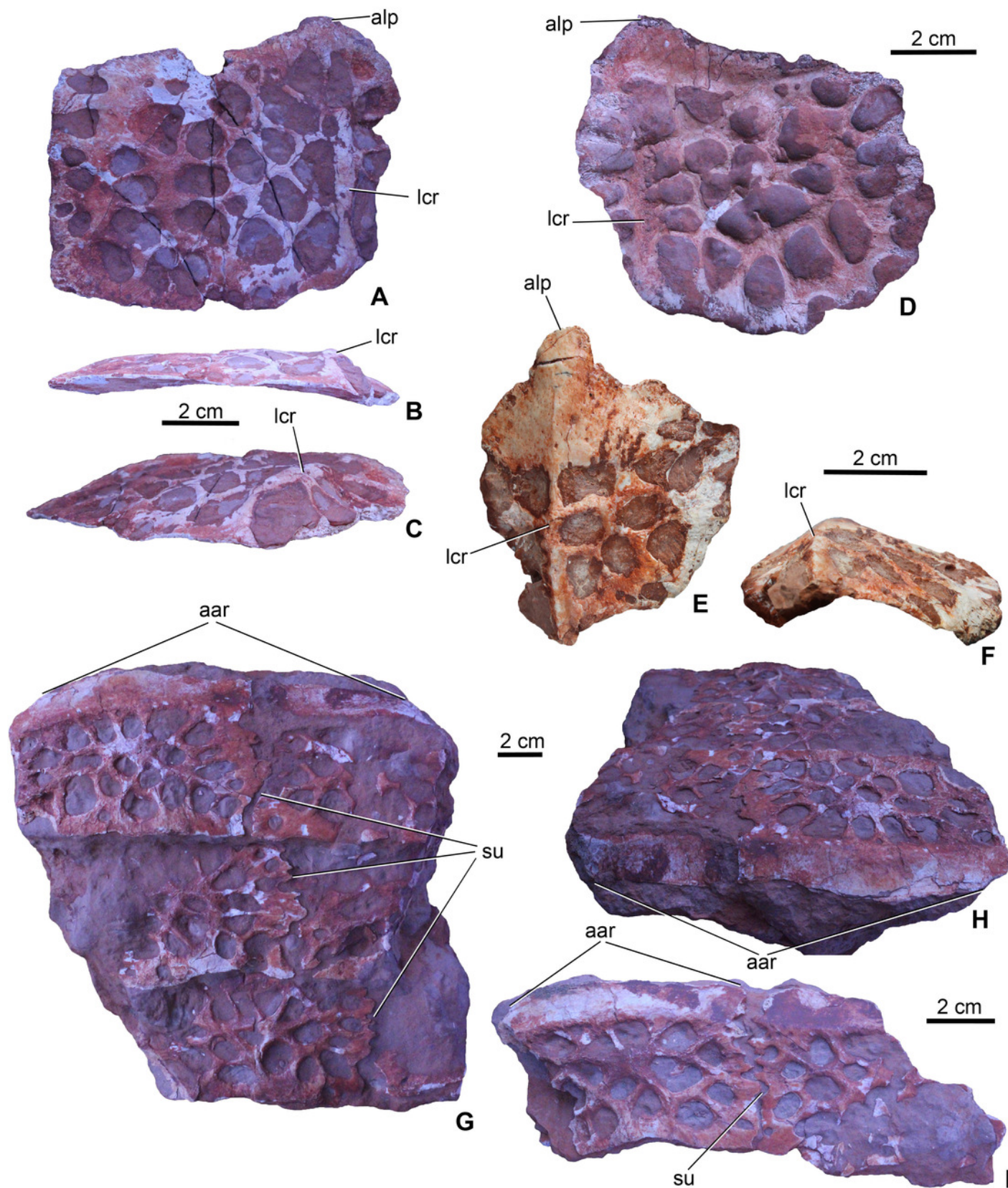
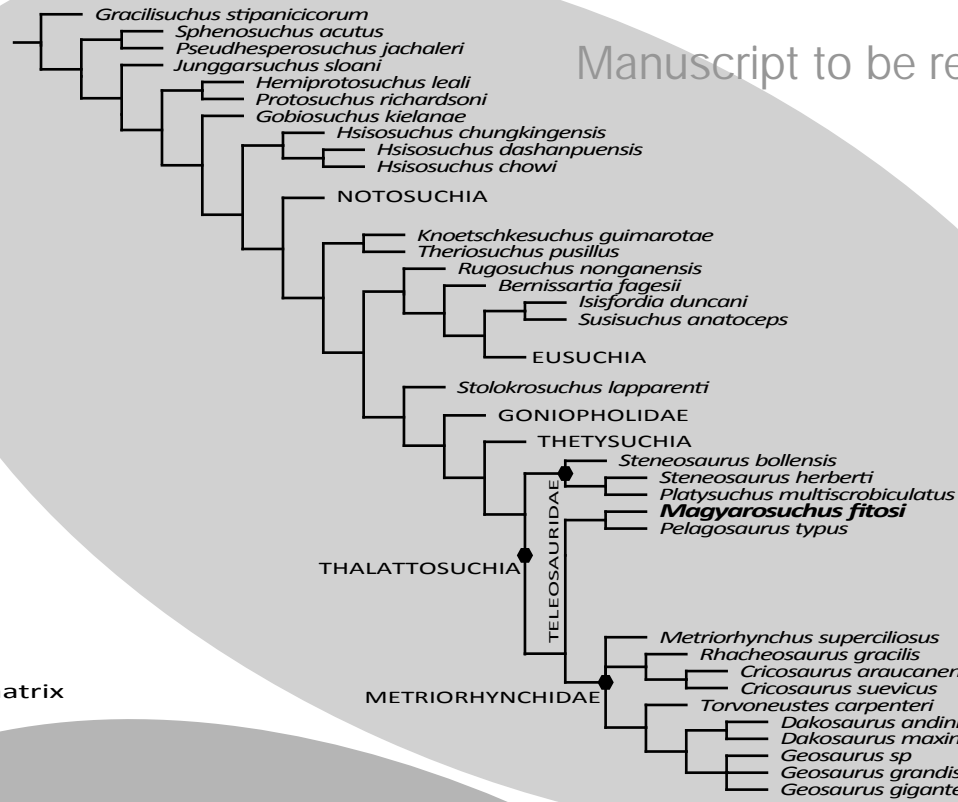


Figure 10(on next page)

Results of the phylogenetic analyses.

A, Strict consensus of 84 most parsimonious cladograms based on the Hastings + Young matrix (Young et al., 2016), showing the phylogenetic relationships of *Magyarosuchus fitosi* gen. et sp. nov. within Metriorhynchoidea. B, Strict consensus of 16 most parsimonious cladograms based on the modified Andrade matrix (Andrade et al., 2011), showing the phylogenetic relationships of *Magyarosuchus fitosi* gen. et sp. nov. within Metriorhynchoidea.



Modified Andrade matrix

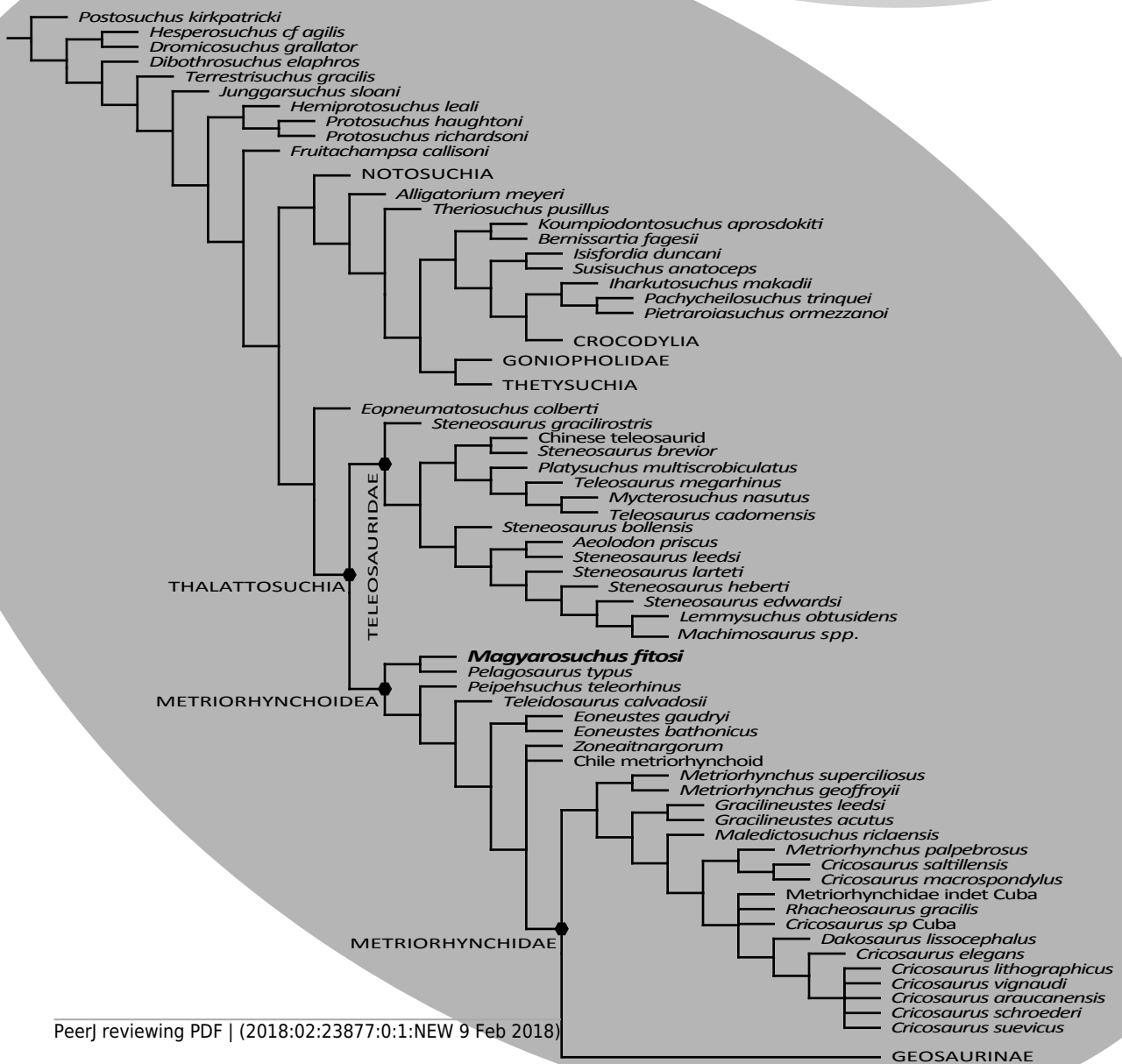


Figure 11(on next page)

Strict consensus of six most parsimonious cladograms based on the Wilberg matrix (Wilberg, 2017), showing phylogenetic relationships of *Magyarosuchus fitosi* gen. et sp. nov. within Metriorhynchoidea.

Wilberg matrix

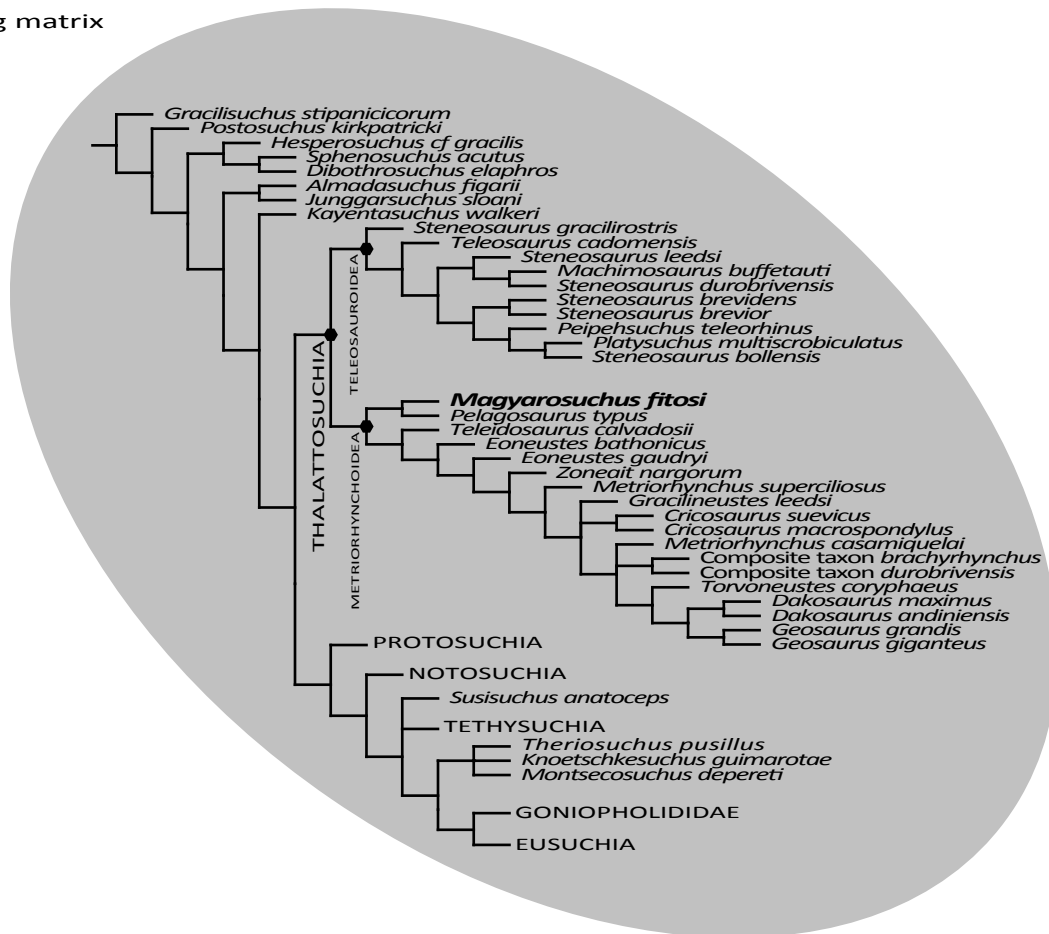
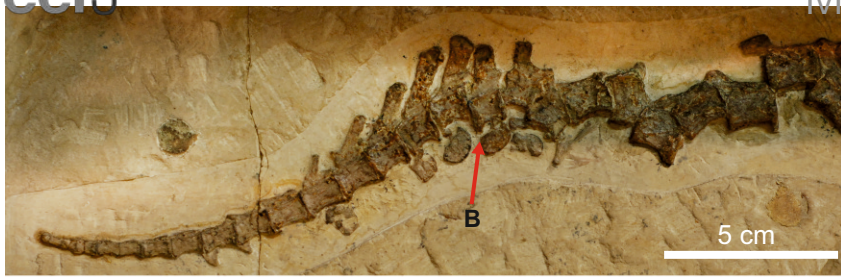


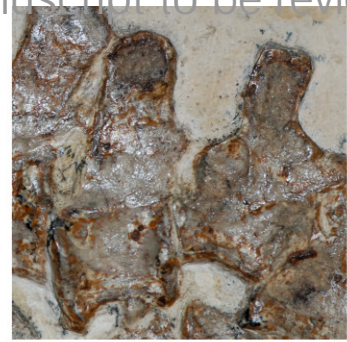
Figure 12(on next page)

Comparison of thalattosuchian bony tails and the distal caudal vertebrae within the bending zone.

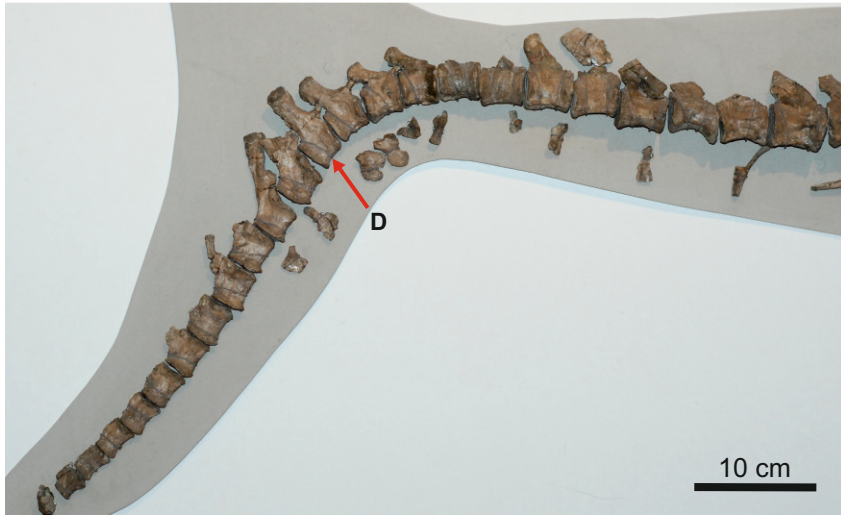
A-B, *Cricosaurus suevicus* from Nusplingen (GPIT RE 7322); C-D, *Metriorhynchus superciliosus* (GPIT RE 9405); E-F, *Steneosaurus bollensis* (MTM M 69242) ; G-H, *Pelagosaurus typus* (MTM M 62 2516); I, *Magyarosaurus fitosi* gen. et sp. nov. distal caudal (MTM V.97.19.) with the interpreted original outline of the vertebra.



A



B



C



D



E



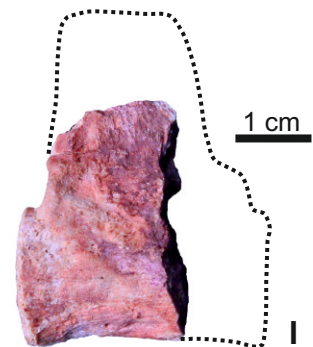
F



H



G



I

Table 1(on next page)

Measurements of the bones of *Magyarosuchus fitosi* gen. et sp. nov. from the Toarcian of the Gerecse Mountains, Hungary.

Measurements of the bones of *Magyarosuchus fitosi* gen. et sp. nov.

Specimen No.	Skeletal element	Greatest diameter (mm)
V.97.2A	dentale fragment	143
V.97.2B	left dentale posterior fragment	171
V.97.2C	mandibula fragment	128
V.97.40	left angular-surangular	106
V.97.26	dorsal vertebra	68
V.97.26	dorsal vertebra	67
V.97.30	last dorsal vertebra	58
V.97.30	first sacral vertebra	60
V.97.30	second sacral vertebra	58
V.97.30	first caudal vertebra	53
V.97.29	proximal caudal vertebra	60
V.97.27	mid-caudal vertebra	61
V.97.28	mid-caudal vertebra	63
V.97.28	mid-caudal vertebra	63
V.97.28	mid-caudal vertebra	61
V.97.28	mid-caudal vertebra	62
V.97.27	fragmentary distal caudal vertebra	58
V.97.27	distal caudal vertebra	61
V.97.27	distal caudal vertebra	63
V.97.27	distal caudal vertebra	62
V.97.21	distal caudal vertebra	62
V.97.21	distal caudal vertebra	64
V.97.22	distal caudal vertebra	63
V.97.31	distal caudal vertebra	60
V.97.31	distal caudal vertebra	59
V.97.31	distal caudal vertebra	63
V.97.31	distal caudal vertebra	59
V.97.19	last caudal vertebra	23
V.97.37	sacral rib with crest	74
V.97.39	sacral rib	75
V.97.7	right coracoideum, fragment with coracoid foramen	66
V.97.7	right coracoideum, distal half	80
V.97.34	left ilium	117
V.97.35	right pubis	164
V.97.49	distal half of left pubis	103
V.97.36	left ischium	137
V.97.44	right ilium	97
V.97.33	right femur	360
V.97.13	left femur	355
V.97.69	left tibia	213
V.97.9	right tibia	210
V.97.15	proximal fibula	62
V.97.45	metatarsal	61
V.97.10	metatarsal III	127
V.97.11	metatarsal	72
V.97.12	tarsus	36
V.97.38	ventral osteoderm	77
V.97.59	dorsal osteoderm	92
V.97.60	dorsal osteoderm	89